

# KUDA: Knowledge Unlearning by Deviating Representation for Large Language Models

Ce Fang<sup>1</sup>, Zhikun Zhang<sup>1</sup>, Min Chen<sup>2</sup>, Qing Liu<sup>1</sup>, Lu Zhou<sup>3</sup>, Zhe Liu<sup>1#</sup>, Yunjun Gao<sup>1#</sup>,

<sup>1</sup>Zhejiang University    <sup>2</sup>Vrije Universiteit Amsterdam

<sup>3</sup>Nanjing University of Aeronautics and Astronautics

## Abstract

*Large language models* (LLMs) acquire a large amount of knowledge through pre-training on vast and diverse corpora. While this endows LLMs with strong capabilities in generation and reasoning, it amplifies risks associated with sensitive, copyrighted, or harmful content in training data. LLM unlearning, which aims to remove specific knowledge encoded within models, is a promising technique to reduce these risks. However, existing LLM unlearning methods often force LLMs to generate random or incoherent answers due to their inability to alter the encoded knowledge precisely. To achieve effective unlearning at the knowledge level of LLMs, we propose *Knowledge Unlearning by Deviating representAtion* (KUDA). We first utilize causal tracing to locate specific layers for target knowledge storage. We then design a new unlearning objective that induces the model’s representations to deviate from its original position in the phase of knowledge removal, thus disrupting the ability to associate with the target knowledge. To resolve the optimization conflicts between forgetting and retention, we employ a relaxation null-space projection mechanism to mitigate the disruption to the representation space of retaining knowledge. Extensive experiments on representative benchmarks, WMDP and MUSE, demonstrate that KUDA outperforms most existing baselines by effectively balancing knowledge removal and model utility retention.

## 1 Introduction

*Large language models* (LLMs) have demonstrated great potential across various domains, such as scientific research [38], education [67], and economics [34]. These capabilities stem from the process of pre-training, during which LLMs learn and store extensive knowledge from diverse corpora [32, 76]. However, the training corpora are primarily collected from the Internet, which may contain sensitive personal information, dangerous knowledge, or copyrighted content [25, 56]. This

raises societal safety concerns, as there is growing awareness that LLMs have a potential risk of being misused [6, 10, 43, 44]. Alignment training [45] represents the mainstream solution for safety risks. However, the phenomenon of shallow alignment [47] renders such approaches inherently vulnerable to adversarial attack. To achieve thorough safety, *LLM unlearning* has emerged as a promising technique by removing the undesired knowledge stored in LLMs’ parameters [36, 52].

**Existing Solutions.** The mainstream unlearning methods for LLMs are to delete or suppress target knowledge that is encoded in LLMs through updating parameters [36, 49, 52]. The *full parameter updates* methods update all parameters that lead LLMs to generate uncontrolled responses when queries are related to sensitive personal information or dangerous knowledge, which we refer to as *target knowledge* [14, 27, 78]. However, the indiscriminate updates risk severe degradations of model utility [52]. Furthermore, the response-oriented methods merely achieve response-level mitigation without inherently removing the target knowledge encoded in the model’s parameters [22, 52, 77]. This renders the removed knowledge easily restored with specific prompts [77].

In comparison, the *partial parameter updates* approaches only update a portion of parameters to reduce the impact on model utility. Nevertheless, they design the parameter selection and removal algorithm independently, failing to tradeoff the target knowledge removal and model utility retention [13, 73]. Concretely, these methods either employ well-designed localization approaches to identify knowledge-relevant parameters and directly apply loss functions from full parameter updates [30, 72], or introduce fine-grained removal algorithms yet rely on empirical results for parameter selection [32]. Therefore, there is a pressing need for a fine-grained, holistic approach that synergistically couples parameter selection and knowledge removal to achieve the balance between target knowledge removal and model utility retention.

**Our Proposal.** To this end, we propose *Knowledge Unlearning by Deviating representAtion* (KUDA), which synergizes parameter selection with knowledge removal based

<sup>#</sup>Corresponding authors.

on the *knowledge storage* property of LLMs. Specifically, the *feed-forward neural network* (FFN) components at specific layers are responsible for storing knowledge learned from training corpora [18], whereas the *multihead self-attention* (MHSA) components at some layers primarily facilitate semantics aggregation [17]. Therefore, by applying updates exclusively to FFNs specialized for knowledge storage, while preserving MHSA components intact, we can remove target knowledge encoded in parameters, with minimal degradation to the LLMs’ general capabilities. However, related works merely confine updates to FFNs’ parameters [32, 72], lacking a synergy pipeline that integrates parameter selection and knowledge removal.

To bridge this gap, KUDA establishes a partial parameter updates unlearning method operating in the representation space. KUDA begins with a component-level identification method, consisting of causal tracing [40] and the metric causal effect, to pinpoint layers whose FFNs exhibit a significant contribution to knowledge storage. Subsequently, a sliding window search strategy is employed to determine unlearning layers, whose a subset of parameters is then designated for unlearning updates. Building upon the selected layers, KUDA implements knowledge removal by intervening in the corresponding *representations* (i.e., the *activation outputs of models’ intermediate layers*). Since knowledge stored in FFNs is activated and incorporated into representations during generation [11], we design a knowledge removal loss function, which induces deviation to push the representation of target knowledge away from its original state. This disrupts the model’s ability to utilize the knowledge for generation. Simultaneously, a constraint loss is introduced to retain the models’ utility. Besides, we depart from the conventional use of a scaling factor to balance knowledge removal and utility retention, as it fails to reconcile the directional conflicts inherent between the two objectives. Instead, we exploit the invariance of null-space. By projecting the unlearning gradients into a relaxation null-space, KUDA eliminates gradient components detrimental to model utility, thereby removing target knowledge while preserving the models’ capabilities. Moreover, we propose a two-stage tuning strategy for the hyperparameter configuration by transforming the joint optimization into two decoupled linear searches.

**Evaluation.** We conduct experiments on two representative benchmarks to illustrate the superiority of KUDA. First, we showed that KUDA achieves a good trade-off between knowledge removal and utility retention. For instance, while achieving near-complete removal of target knowledge, KUDA incurs marginal utility degradations of only 3.1% on MUSE and 1.7% on WMDP. In addition to unlearning performance, KUDA demonstrates robust model generalizability, seamlessly extending its unlearning capabilities to modern models like Llama-3.1 and Qwen-3. From the perspective of gradient dynamics, we further reveal that KUDA balances removal and retention by maintaining near-orthogonal gradient directions

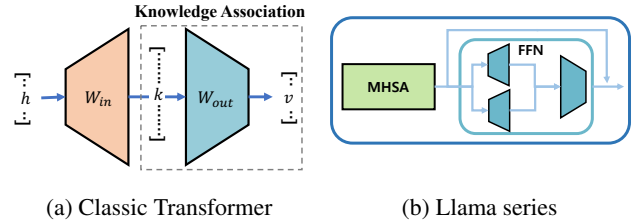


Figure 1: FFN architectures in Transformer-based models.

between the two objectives, thereby preventing significant conflicts. Moreover, we demonstrate the complex coupled impact of two influential hyperparameters, i.e., the inverse unlearning temperature and the null-space relaxation threshold, thus necessitating our decoupled search strategy.

**Contributions.** Our contributions are three-folds:

- Grounded in the LLMs’ knowledge storage property, we propose a representation-level unlearning method that integrates *unlearning layer selection*, *representation deviation*, and *relaxation null-space projection*. By applying stable updates to parameters correlated with knowledge storage, KUDA achieves precise knowledge removal while retaining the LLMs’ utility effectively.
- By identifying the stability boundary, we introduce a two-stage tuning strategy that simplifies the complex joint hyperparameter optimization into two decoupling linear searches. This facilitates the practical deployment across datasets.
- We conduct extensive experiments to demonstrate the unlearning performance of KUDA. Furthermore, we provide mechanistic insights into gradient dynamics, revealing that KUDA mitigates unlearning conflicts by maintaining near-orthogonal gradients.

## 2 Preliminary

### 2.1 Large Language Models

Transformer-based LLMs achieve context understanding and text generation with two crucial mechanisms: FFN-based associative memory and MHSA-driven contextual interaction [18]. Concretely, FFN acts as a knowledge storage repository [18, 40], whereas MHSA facilitates the semantics aggregation [17].

**FFN for Knowledge Storage.** FFN can be modeled as a *two-layer key-value knowledge storage* [40], as illustrated in Figure 1a. Given an input, the first-layer  $W_{in}$  generates a *key* based on the input; the second-layer  $W_{out}$  maps the key to the stored knowledge related to that input, and generates a corresponding *value*. This knowledge-retrieval process incorporates rich knowledge into hidden representations to influence

the final text generation, which can be formally formulated as:

$$\begin{aligned} k_i^l &= \sigma(W_{in}^l(h_i^{l-1})), \\ v_i^l &= W_{out}^l \cdot k_i^l, \end{aligned}$$

where  $l$  and  $i$  represent the layer index and the token position, and  $\sigma$  denotes the activation function, such as ReLU.  $W_{in}$  and  $W_{out}$  are two-layer linear transformation matrices.

For more recent LLMs, such as Llama [63], that adopt the advanced FFN variants, the mechanism of knowledge storage remains functionally equivalent. As presented in Figure 1b, this FFN consists of three linear transformation matrices ( $W_{gate}$ ,  $W_{down}$ , and  $W_{up}$ ), and the process of generating value can be represented as:

$$v_i^l = W_{down}^l \cdot [\text{Swish}(W_{gate}^l(h_i^{l-1})) \otimes W_{up}^l(h_i^{l-1})],$$

where  $\otimes$  is the Hadamard Product and Swish [51] is an activation function. Although differing structurally from the classical FFN, the combined operations of  $W_{gate}$  and  $W_{up}$  can still be regarded as the first-layer to form the key, while  $W_{down}$  serves as the second-layer to transform key to value.

**MHSA for Semantics Aggregation.** MHSA provides LLMs with powerful capabilities of semantics aggregation [17]. On one hand, it aggregates semantic information from preceding tokens to the current position, thus facilitating the awareness of context. On the other hand, it extracts task-relevant knowledge from the representations refined by FFNs’ knowledge storage mechanism. This synergy effect enables LLMs to understand the complex context and utilize the rich knowledge encoded in LLMs’ parameters to generate high-quality text.

## 2.2 Causal Tracing

*Causal tracing* [40] is an interpretability method to quantify the importance of activations across layers and components for generating accurate output. The workflow mainly contains three stages:

**Clear Run.** The objective is to collect the original states of text generation. We execute a forward pass with the given prompts to collect activations across all components, denoted as  $H = \{h_{m,i}^l \mid m \in \{\text{MHSA}, \text{FFN}, \text{Layer}\}\}$ , where  $l$  is the layer index and  $i$  is the token position. Simultaneously, we record the probability  $\mathbb{P}[t_{a_1}]$  of the model correctly predicting the first answer token  $t_{a_1}$ .

**Corrupted Run.** The objective is to collect the corrupted states with the perturbed input embedding. We add perturbing noise to the embedding of input tokens to prevent the model from making a correct prediction. Corresponding to “Clear Run,” collect the activations  $H^*$  and the probability  $\mathbb{P}^*[t_{a_1}]$  in the current case.

**Corrupted-with-Restoration Run.** The objective is to restore each activation to quantify its importance for the correct

prediction. With the perturbed inputs embedding, we individually replace the activations of each component across layers by the correct state from “Clear Run,” and records the resulting probability  $\mathbb{P}_{m_i}^*[t_{a_1}]$ , where  $m_i^l$  is the restored component type  $m$ , layer  $l$  and token  $i$ .

## 2.3 Null-Space

*Null-space* is an effective technique for enhancing the stability and plasticity of deep learning networks in post-training scenarios [15, 68]. The core idea is to confine parameter updates within the null-space of the input feature space learned from previous tasks, thereby protecting prior knowledge from updated parameters.

For network  $\mathcal{M}$  trained on prior tasks with data  $x_{old}$ , let  $\Delta w^l$  denote the update gradients of a new task applied to parameters  $W_{old}$  at layer  $l$ . When  $\Delta w^l$  lies within the null-space of the *input features space*  $X_{old}^l$  of previous tasks, there is  $\Delta w^l \cdot x_{old}^l = 0$  [68]. This property prevents detrimental disruption to the representations at layer  $l$  learned from previous tasks during continual learning:

$$(W_{old}^l + \Delta w^l) \cdot x_{old}^l = W_{old}^l \cdot x_{old}^l + 0 = y_{old}^l$$

Therefore, constraining gradients in such null-space could preserve the integrity of the model’s previous foundational capabilities:

$$\mathcal{M}(x_{old}, W_{old}) = \mathcal{M}(x_{old}, W_{new}) = y_{old}$$

where  $W_{new} = W_{old} + \Delta w$ . Briefly, when updates are constrained in the null-space of input features of layer  $l$ , the outputs at  $l$  for previous tasks remain “invariant” despite the updated parameters.

## 3 Problem Statement and Existing Solution

### 3.1 Problem Formulation

LLM unlearning is defined as the process of selectively removing target knowledge from a pre-trained LLM  $\mathcal{M}_\theta$ , which is trained on dataset  $\mathcal{D}$ . Let  $\mathcal{D}_f \subset \mathcal{D}$  be the target subset of data to be removed, which is referred to as “*forgetting knowledge*” or “*forgetting set*.” Correspondingly,  $\mathcal{D}_r = \mathcal{D} \setminus \mathcal{D}_f$  is denoted as retained data, referred to as “*retaining knowledge*” or “*retaining set*”. Formally, the objective of LLM unlearning is to derive an unlearned model  $\mathcal{M}_{\theta'}$  whose behaviors are consistent with the model  $\mathcal{M}_{re}^{\mathcal{D}_r}$  retrained on  $\mathcal{D}_r$ :

$$\mathcal{M}_{\theta'}(y \mid x) \approx \mathcal{M}_{re}^{\mathcal{D}_r}(y \mid x), \quad \forall (x, y) \in \mathcal{D},$$

where  $\mathcal{M}_{re}^{\mathcal{D}_r}$  is considered as the *golden baseline* unlearned model. Briefly, LLM unlearning is the process of removing knowledge from  $\mathcal{D}_f$  while retaining knowledge from  $\mathcal{D}_r$ .

## 3.2 Existing Solution

**GA [27].** *Gradient ascent* (GA) is the most representative method for LLM unlearning. The general idea is to perform reverse optimization (gradient ascent instead of descent) on  $\mathcal{D}_f$ , rewarding LLMs to produce incorrect outputs. Concretely, GA can be formulated as *maximizing* the negative log-likelihood loss:

$$\mathcal{L}_{GA} = \mathbb{E}_{\mathcal{D}_f} [\sum \log (p_{\theta}(x_t | x_{<t}))],$$

where  $p_{\theta}(x_t | x_{<t})$  is the prediction probability of token  $x_t$  calculated by LLM with parameters  $\theta$  and input tokens  $x_{<t}$ .

However, directly training with  $\mathcal{L}_{GA}$  could cause severe model collapse [78]. To address this, *gradient difference* (GradDiff) [39] introduces a constraint term (referred to as retaining loss  $\mathcal{L}_r$ ) on  $\mathcal{D}_r$  to prevent excessive forgetting. The weighted sum constitutes the formal unlearning objective [74]:

$$\mathcal{L}_u = \mathcal{L}_f(x \in \mathcal{D}_f; \theta) + \alpha \mathcal{L}_r(x \in \mathcal{D}_r; \theta),$$

where  $\mathcal{L}_f = \mathcal{L}_{GA}$ , and  $\alpha$  is a scaling factor for the balance between forgetting and retention.

**NPO [78].** *Negative preference optimization* (NPO) is an alternative to GA. Inspired by DPO [50], NPO regards the forgetting data as negative samples, and facilitates forgetting by penalizing the model for generating the dispreferred data:

$$\mathcal{L}_{NPO}(\theta) = -\frac{2}{\beta} \mathbb{E}_{\mathcal{D}_f} \left[ \log \sigma \left( -\beta \log \frac{\pi_{\theta}(y | x)}{\pi_{ref}(y | x)} \right) \right],$$

where  $\sigma(\cdot)$  is the sigmoid function, and  $\pi_{ref}$  and  $\pi_{\theta}$  denote the original and the unlearned model, respectively. In comparison with GA, NPO resolves the absence of an optimization lower bound and exhibits a slower divergence rate, leading to a more stable unlearning process.

**RMU [32].** *Representation misdirection for unlearning* (RMU) is the state-of-the-art method of partial parameter updates. It suppresses the generation of target knowledge by driving the internal activations of empirically selected layers towards a random uniform distribution, formulated as:

$$\mathcal{L}_{RMU} = \mathbb{E}_{\mathcal{D}_f} [\|a_f(x) - c \cdot u\|_2^2] + \alpha \cdot \mathbb{E}_{\mathcal{D}_r} [\|a_f(x) - a_r(x)\|_2^2],$$

where  $u$  is a random vector, and  $a$  represents the activations.  $c$  and  $\alpha$  denote a forgetting coefficient and a scaling factor. RMU achieves knowledge removal by disrupting the original activations of forgetting data, while retaining model utility by enforcing activation consistency on retaining data.

**Drawbacks of Existing Solutions.** The methods of full parameter updates exhibit a significant advantage in knowledge removal by deliberately inducing the generation of random responses. However, given that all parameters are updated indiscriminately, they frequently result in irreversible utility degradation or complete model collapse, and may

only achieve response-level mitigation instead of removing knowledge encoded in parameters. Conversely, partial parameter updates methods prioritize utility retention yet often fail to achieve satisfactory effectiveness of knowledge removal [13, 73]. This deficiency primarily stems from a weak coupling between the parameter selection and the knowledge removal algorithm. While the property of knowledge storage offers a promising design perspective, related efforts remain confined to restricting updates to FFNs’ parameters, lacking a synergetic design that aligns the entire pipeline with such a property. For instance, RMU induces divergence in intermediate activations to remove knowledge, yet its parameter selection relies on the empirical search.

## 4 KUDA

### 4.1 Intuition

As detailed in Section 2.1, FFNs act as *knowledge storage* by activating relevant knowledge stored in parameters to influence the generation. We define the transition process from key to value as “*knowledge association*” (Figure 1a), as this stage achieves the retrieval of relevant knowledge based on input tokens. Through this, the representations contain not only the semantic context of the inputs but also their associations with relevant knowledge.

This property implies a viable pathway for controllable knowledge removal by perturbing the knowledge associations in specific FFNs to disrupt the generation of target knowledge. It enables a selective update strategy that focuses modifications on the FFNs responsible for knowledge storage, while leaving the MHSA components specific to semantics aggregation entirely intact. Consequently, this achieves target knowledge removal while robustly maintaining model utility by preserving the core semantic capabilities of the MHSA.

While conceptually intuitive, the direct quantification and modification of target knowledge encoded in FFNs remains a formidable challenge. However, since representations encapsulate both input semantics and their associations with relevant knowledge [11, 17], they offer a more accessible pathway for intervening in knowledge associations. Consequently, we propose a representation-based unlearning method, named *Knowledge Unlearning by Deviating representation* (KUDA), to disrupt the utilization of target knowledge for generation.

### 4.2 Overview

KUDA aims to leverage the property of knowledge storage in Transformer-based models [18, 40] for LLM unlearning. To remove knowledge stored in FFNs, KUDA employs selective parameter updates that deviate the representations of target knowledge away from their original states. The pipeline is illustrated as Figure 2.

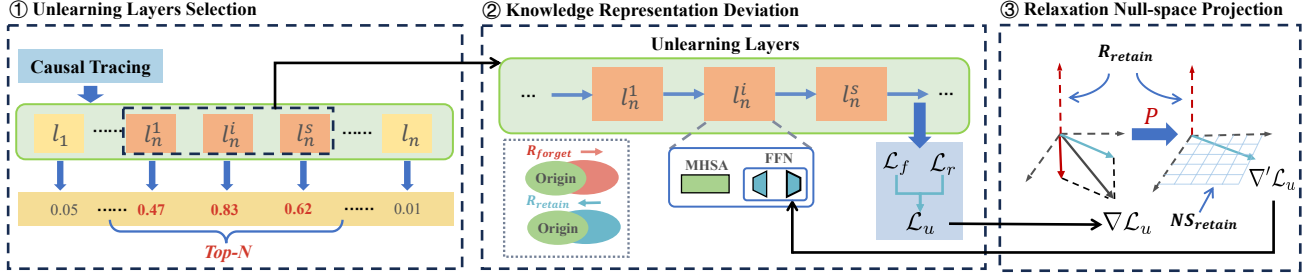


Figure 2: The overview of KUDA pipeline to balance the knowledge removal and utility retention for LLMs. KUDA includes three major stages: 1) We employ causal tracing and causal effect to identify FFNs critical for knowledge storage, and apply a sliding window to select the target *unlearning layers* for parameter updates. 2) The representations generated from the last unlearning layer are captured and utilized to derive the update gradients  $\nabla \mathcal{L}_u$  based on the mechanism of *knowledge representation deviation*. 3) The gradients are projected into the *relaxation null-space* of retaining knowledge, and  $\nabla' \mathcal{L}_u$  is then applied to the last linear transformation matrix of FFN in each unlearning layer.  $R_{forget}$  and  $R_{retain}$  are the representations of forgetting and retaining knowledge.  $NS_{retain}$  denotes the relaxation null-space of retaining knowledge.

**Step 1: Unlearning Layers Selection.** Our approach begins by identifying layers whose FFNs are specialized in knowledge storage. To this end, we employ causal tracing [40] and define a metric named causal effect to achieve a component-level identification. Based on causal effect, we propose a sliding window search strategy to select unlearning layers, a portion of whose parameters is the targets for subsequent updates. We refer the readers to Section 4.3 for more details.

**Step 2: Knowledge Representations Deviation.** Knowledge stored in FFN parameters is retrieved and incorporated into representations through knowledge association. Building upon this, we design a knowledge removal loss, which involves inducing the representation of target knowledge away from its original state. This deviation perturbs the established knowledge associations, thereby disrupting the generation of target knowledge. Besides, a constraint loss is also introduced for retention. The detailed design of unlearning objectives is presented in Section 4.4.

**Step 3: Null-space Projection.** To address directional conflicts between forgetting and retention, we introduce relaxation null-space projection to eliminate the unlearning gradient components (derived from Step 2) that compromise model utility. Moreover, we propose stochastic proportional sampling to resolve computational bottlenecks and introduce the relaxation threshold to prevent excessive suppression to the knowledge removal process. The projected gradients preserve utility without compromising the effectiveness of forgetting. See Section 4.5 for more details.

### 4.3 Unlearning Layers Selection

KUDA begins by identifying the LLM layers whose FFNs are predominantly responsible for storing knowledge, which subsequently guides the selection of parameters for updates.

**Causal Effect.** Previous studies on layer selection for un-

learning primarily focused on either the entanglement degree between forgetting and retaining knowledge [46], or on the layer’s correlation with the LLMs’ refusal behaviors [55]. However, these coarse layer-level granularity methods overlook the functional distinctions between layer-internal components. Concretely, the contributions of MHSA and FFN are merged by residual connection, rendering the selection results of these methods invariably influenced by both components simultaneously. This indicates that selected layers may be critical for semantics processing dominated by MHSA [16, 20, 28], instead of those driven by FFNs for knowledge storage (see Section 2.1 for more details). Therefore, the coarse-grained selection may inadvertently damage the models’ capabilities of context-awareness or text generation.

To leverage the knowledge storage property of LLMs, we propose a fine-grained, component-level identification method. Specifically, we identify layers whose FFNs exhibit specialization in knowledge storage, which allows decoupling of MHSA and FFN during layer selection. This motivates the adoption of *causal tracing*, which quantifies the contribution of each intermediate activation, as detailed in Section 2.2. After performing causal tracing, we define the average probability difference between “Corrupted Run” and “Corrupted-with-restoration Run” as *Causal Effect* ( $CE_m^l$ ), to reveal the importance of components  $m$  at layer  $l$  for correct generation:

$$CE_m^l = \frac{1}{B \cdot T} \sum_{i=1}^B \sum_{j=1}^T (\mathbb{P}_{m_i}^* - \mathbb{P}^*), \quad (1)$$

where  $B$  and  $T$  represent the input batch size and sequence length. Concretely, a higher  $CE_{FFN}^l$  score reflects that the FFN significantly contributes to knowledge storage during the generation process.

Ideally, causal tracing should be performed on task-specific datasets, such as  $\mathcal{D}_f$  or  $\mathcal{D}_r$ , to pinpoint FFNs storing target knowledge. However, as presented in Section 5.6, the sub-

---

**Algorithm 1** Sliding Window Search

---

**Require:** Scores  $\{\text{CE}_{FFN}^l\}$ , candidate size  $N$ , window size  $s$

**Ensure:** Selected unlearning layers  $\mathcal{W}_{un}$

```
1:  $\mathcal{S}_{top} = \{l_{(1)}, \dots, l_{(N)} \mid \text{rank}(\text{CE}_{FFN}^l) \leq N, (1) \prec \dots \prec (N)\}$ 
2:  $p \leftarrow \lceil s/2 \rceil$   $\triangleright$  Position of  $l_{(i)}$  as the window center
3: for  $i = \lceil (N+1)/2 \rceil$  to  $N$  do
4:    $l_j \leftarrow \mathcal{S}_{top}(i)$ 
5:    $\mathcal{W}_{j,s} \leftarrow \{l_{j-p+1}, \dots, l_{j-1}, l_j, l_{j+1}, \dots, l_{j+s-p}\}$ 
6:   if  $\text{HR}(\mathcal{W}_{j,s}) > 0.5$  then  $\triangleright$  Hit Ratio condition
7:     return  $\mathcal{W}_{un} \leftarrow \mathcal{W}_{j,s}$ 
8:   end if
9: end for
10: return  $\mathcal{W}_{\lceil (N+1)/2 \rceil, s}$ 
```

---

stantial computational overhead of causal tracing renders it impractical to calculate CE for different unlearning datasets. Therefore, we execute causal tracing *only once per model* using “1,000 factual statements [40].” Since this dataset contains a wide range of knowledge domains, the calculated CE scores exhibit generalizability across topics and thus can be reused to mitigate requirements for causal tracing in future unlearning tasks.

**Selection Strategy.** Based on empirical investigation, we observe that though with high  $\text{CE}_{FFN}$  scores, KUDA is sensitive to the layer positions. Concretely, the first several layers of the FFN-dominant zone primarily handle generic features [28], while those layers located at its terminus facilitate the functional transition from knowledge retrieval to semantics aggregation, rendering both of them ill-suited as unlearning layers. Besides, contiguous layers should be prioritized to preserve the coherence of the representation space across layers. See Section C.1 for more detailed analysis.

Therefore, we design a *sliding window search* strategy to select unlearning layers, as presented in Algorithm 1. First, we construct a candidate set  $\mathcal{S}_{top}$  containing  $N$  layers with the highest  $\text{CE}_{FFN}^l$  scores, ordered by layer indices. Starting from the median layer of  $\mathcal{S}_{top}$  and iterating toward the deeper layers, we treat a candidate layer as a centric anchor to bi-directionally expand a sliding window  $\mathcal{W}_{j,s}$  of size  $s$ . The layers within  $\mathcal{W}_{j,s}$  are selected as *Unlearning Layers* only if  $\mathcal{W}_{j,s}$  meets the Hit Ratio (HR) condition:

$$\text{HR}(\mathcal{W}_{j,s}) = \frac{|\mathcal{W}_{j,s} \cap \mathcal{S}_{top}|}{s} > 0.5 \quad (2)$$

With a majority-principle threshold of 0.5, the HR constraint ensures that the window is mainly composed of layers with significant contributions to knowledge storage, filtering out isolated outliers.

## 4.4 Knowledge Representation Deviation

As discussed in Section 4.1, input tokens activate knowledge stored in specific FFNs during generation, establishing associations that are then incorporated, along with the semantic context of inputs, into the hidden representations [18, 40]. For instance, given the input “Apple CEO,” the representations of specific layers might contain the association with “Tim Cook,” which is the implicit knowledge stored in FFNs and triggered by the input context. Such knowledge associations refine the information of representations and are subsequently extracted by MHSA to influence the final output [17]. Therefore, disrupting these associations in representations can effectively inhibit the generation of target knowledge, achieving the goal of unlearning. To this end, we design the representation-based objectives for target knowledge removal.

**Forgetting Loss.** Inspired by preference optimization [50, 78], we design a deviation mechanism to push the representation of forgetting knowledge away from its original state. Once the hidden representations are perturbed from their pre-trained state, the incorporated associations with relevant knowledge can no longer be effectively utilized by subsequent layers.

While preference optimization relies on the similarity of model outputs, the lack of a direct mapping between hidden representations and outputs calls for a substitute metric to quantify the similarity of representations. To address this issue, we adopt *cosine similarity* between representations of the unlearning model and the original ones. Given the high dimensionality and sparsity of representations, cosine similarity is particularly well-suited, as it measures direction consistency rather than magnitude and is robust to sparse activation patterns. Besides, its value transition of  $1 \rightarrow 0$  provides a mathematical implication of “reducing similarity.” This process effectively drives the representation away from its original state, intuitively aligning with the goal of preference optimization. Furthermore, we adopt the cosine complement ( $1 - \cos$ ), which enables similarity reduction while simultaneously ensuring the training objective remains convergent. Accordingly, we refine preference optimization by integrating the aforementioned designs to construct the forgetting objective, which induces deliberate deviation in the representations of forgetting knowledge:

$$\mathcal{L}_f = -\frac{2}{\beta} \mathbb{E}_{\mathcal{D}_f} \left[ \log \sigma \left( \beta \cdot \left( 1 - \cos \langle \mathcal{R}_{un}^l(x), \mathcal{R}_{ori}^l(x) \rangle \right) \right) \right] \quad (3)$$

where  $x \in \mathcal{D}_f$  are the forgetting data,  $\cos \langle \cdot \rangle$  denotes the cosine similarity, and  $\sigma(\cdot)$  refers to the sigmoid function. The hyperparameter  $\beta$  represents the inverse unlearning temperature. Notably,  $\mathcal{R}_{un}^l$  and  $\mathcal{R}_{ori}^l$  denote the representations at the *last unlearning layer*  $l'$  from the unlearning and the original models. Since knowledge is distributed across layers and aggregated through residual connections, the representation at layer  $l'$  integrates a substantial amount of forgetting knowledge and corresponding associations. This makes it a principled choice

as the target in  $\mathcal{L}_f$ .

Briefly, the minimization of  $\mathcal{L}_f$  serves to reduce similarity  $\cos(\cdot)$  between the current and original representations. This derives a deviation of the target knowledge representation from its pre-trained state, which inhibits the subsequent generation of that knowledge.

**Retaining Loss.** Update gradients derived from  $\mathcal{L}_f$  often lead to severe degradation of model utility, thus necessitating the incorporation of constraints to ensure a controllable unlearning process [66]. In contrast to output-level unlearning losses that typically employ KL-divergence or cross-entropy to restrict changes in the token probability distributions, these common constraint terms are incompatible with hidden representations, which reside in a continuous vector space rather than a discrete probability space. Consequently, we adopt an  $\ell_2$ -regularization item [8] on  $\mathcal{D}_r$  to effectively penalize excessive deviations within the latent representation space:

$$\mathcal{L}_r = \mathbb{E}_{\mathcal{D}_r} \left[ \ell_2(\mathcal{R}'_{un}(x), \mathcal{R}'_{ori}(x)) \right], \quad (4)$$

where  $x \in \mathcal{D}_r$  are the retaining data, and other symbols are consistent with those defined in  $\mathcal{L}_f$ . Beyond preserving factual knowledge,  $\mathcal{D}_r$  is also essential for retaining the structural knowledge, such as grammatical and syntactic patterns, that form the foundation of the model’s excellent linguistic capabilities [52].

**Unlearning Loss.** The final unlearning loss is formulated as the composite of forgetting and retaining objectives, which are responsible for knowledge removal and utility retention, respectively:

$$\mathcal{L}_u = \mathcal{L}_f + \mathcal{L}_r \quad (5)$$

In contrast to conventional methods, we discard the scaling factor (*i.e.*,  $\mathcal{L}_f + \alpha \cdot \mathcal{L}_r$ ) that is typically employed to balance forgetting and retention. In practice, due to the difference in loss functions and task requirements, the tuning effect of such hyperparameters might be non-linear, and substantially increases the cost of hyperparameter searching in specific tasks. This complexity diminishes the adaptability across diverse unlearning scenarios. We will elaborate on its fundamental limitation and our improvement in Section 4.5.

**Parameter Update.** According to Section 2.1, the *last linear transformation matrix*  $W_{out}$  (referred to as  $W_{down}$  in some LLMs, such as Llama) in FFNs serves a crucial role in knowledge association. Therefore, we intervene in the association process to achieve unlearning by applying parameter updates  $\nabla_w \mathcal{L}_u$  exclusively to  $W_{out}$  of FFNs across *all unlearning layers*, as knowledge is distributed in multiple layers [18]. This selective refinement enables precise removal of target knowledge while preserving model utility.

## 4.5 Relaxation Null-Space Projection

As shown in Section 2.3, null-space has the property of *invariance*, motivating us to adopt this in reconciling the conflicts

between two unlearning targets.

**Drawbacks of Scaling Factor.** The most representative paradigm for utility retention involves incorporating the retaining loss and employs a scaling factor to achieve the trade-off between forgetting and retention, *i.e.*,  $\mathcal{L}_f + \alpha \cdot \mathcal{L}_r$ . However, previous studies [66, 70, 78] have revealed its limited effectiveness in preventing the utility degradation, due to the failure to reconcile the conflict between forgetting and retention. A crucial issue arises when any component of unlearning gradients acts in opposition to the retention direction, as such a component inevitably compromises model utility. This stems from the *directional* conflict that cannot be resolved by merely adjusting the magnitude of gradients through a scaling factor  $\alpha$ .

These limitations motivate a subspace transformation mechanism to eliminate the detrimental influence of gradient components on model utility. The invariance property of null-space provides a solution. Concretely, we project gradients  $\nabla_w \mathcal{L}_u$  into the null-space of the input feature of  $\mathcal{D}_r$  at layer  $l$ . This remains the representations of retaining knowledge *invariant* despite updated parameters, as introduced in Section 2.3.

**Input Feature Capturing.** First, we compute the uncentered covariance statistic of  $k$  to characterize the input feature space of retaining knowledge in  $W_{out}$ , where  $k$  is the input of  $W_{out}$  as described in Section 2.1. The covariance captures correlations across feature dimensions. Concretely, we input retaining data  $x_r \in \mathcal{D}_r$  to the original model to get the input  $k_r^l$  of  $W_{out}^l$  across all unlearning layers. The uncentered covariance statistic  $\mathcal{K}_r^l \in \mathbb{R}^{d \times d}$  is denoted as the input feature space and formulated as:

$$\mathcal{K}_r^l = \frac{1}{n_r} \sum_{i=1}^{n_r} (k_{r,i}^l)^\top k_{r,i}^l \quad (6)$$

However, this phase requires  $|\mathcal{D}_r|$  times of forward passes to capture the input features, which limits the scalability in the practical large-scale retaining dataset. Therefore, we propose *Stochastic Proportional Sampling*, which constructs an approximate input feature space using a sampled subset  $\hat{\mathcal{D}}_r$ :

$$\hat{\mathcal{D}}_r = \{x_{r_i} \mid i \sim \text{Uniform}(1, |\mathcal{D}_r|), \text{ s.t. } |\hat{\mathcal{D}}_r| = p\% \cdot |\mathcal{D}_r|\}, \quad (7)$$

where  $p$  is the sampling ratio. This stochasticity ensures the statistical representativeness of the captured feature distribution, while the proportional sampling effectively reduces computational overhead by reducing the number of required forward passes.

**Null-Space Relaxation.** Next, we apply *singular value decomposition* (SVD) to  $\mathcal{K}_r^l$  to identify feature directions that are uncorrelated with retaining knowledge:

$$U^l, \Lambda^l, (U^l)^\top = \text{SVD}(\mathcal{K}_r^l), \quad (8)$$

where the subset of singular vectors  $U_z^l \subset U^l$ , corresponding to zero singular values, constitute the *strict null-space*.

Then, the gradients are projected into the null-space of retaining knowledge via the *strict null-space projection matrix*  $U_z^l(U_z^l)^\top$ . However, given the representation *entanglement* between the forgetting and retaining knowledge, such a strict projection matrix inadvertently constrains the updates to representations of forgetting knowledge, thereby hindering the thorough removal.

To this end, we introduce a *null-space relaxation threshold*  $\tau$  to relax the strict zero-singular-value constraint. Specifically, we construct an approximate null-space by selecting singular vectors whose corresponding singular values fall below  $\tau$ :

$$\mathcal{N}_\tau^l = \left\{ u_i^l \mid \lambda_i^l < \tau, \lambda_i^l \in \Lambda, u_i^l \in U^l \right\}, \quad (9)$$

Based on this, the *Relaxation Null-Space Projection Matrix* is then defined as  $P_\tau^l = \mathcal{N}_\tau^l(\mathcal{N}_\tau^l)^\top \in \mathbb{R}^{d \times d}$ . This tolerates updates in directions weakly correlated with retaining knowledge, thus removing target knowledge without incurring significant degradation to utility.

**Gradients Projection.** Finally, before updating parameters, we project the gradients into the relaxation null-space of retaining knowledge with  $P_\tau$ , ensuring that the update gradients do not interfere with content generation related to retaining knowledge:

$$\nabla'_{w^l} \mathcal{L}_u = P_\tau^l \cdot \nabla_{w^l} \mathcal{L}_u, \quad (10)$$

where  $\nabla'_{w^l} \mathcal{L}_u$  is adopted to update  $W_{out}^l$  at layer  $l$  for unlearning.

## 4.6 Principled Hyperparameter Configuration

The unlearning performance of KUDA is mainly influenced by the inverse unlearning temperature ( $\beta$ ) and the null-space relaxation threshold ( $\tau$ ).  $\beta$  controls the intensity of forgetting and enhances knowledge removal when decreasing. A smaller  $\tau$  results in feature directions less correlated with retaining knowledge, thereby enhancing utility retention while weakening forgetting. As such, we propose a *two-stage tuning* strategy for practical deployment:

- 1) **Stability Boundary Identification.** We fix  $\beta = 0.1$  to enforce a state of over-forgetting. Maintaining maximal forgetting, we decrease  $\tau$  to identify an inflection point, at or below which knowledge removal is substantially weakened, as illustrated in [Figure 9](#). We designate this specific  $\tau$  as the *stability boundary*, with further details provided in [Section C.2](#).
- 2) **Unlearning Balance.** Building upon the identified boundary, we select a  $\tau$  slightly larger than this boundary to ensure the effectiveness of removal, and then increase  $\beta$  across  $\{0.1, 1.0, 2.0\}$ . This process mitigates forgetting intensity to balance knowledge removal and utility retention. The principled strategy prioritizes the stability boundary of representation space under an extreme forgetting scenario

and then refines the unlearning balance, thereby transforming a complex joint optimization into two sequential one-dimensional searches.

## 5 Evaluation

### 5.1 Experimental Setup

There are multiple well-established benchmarks for evaluating the performance of various LLM unlearning algorithms. These benchmarks incorporate a set of datasets, metrics, and models. In this paper, we evaluate the performance of KUDA on two representative benchmarks, MUSE [58] and WMDP [32].

**Datasets.** The datasets consist of *forgetting set* and *retaining set*.

- **MUSE.** It consists of two datasets, BOOKS and NEWS. For BOOKS, the forgetting set comprises text excerpts from the Harry Potter series, while the retaining set is sampled from the Harry Potter Fandom Wiki. For NEWS, the forgetting and retaining sets are constructed by randomly partitioning BBC News articles published after August 2023.
- **WMDP.** It focuses on the malicious misuse of hazardous knowledge in LLMs, aiming to evaluate the ability to remove dangerous knowledge from models. Its forgetting set comprises harmful knowledge in Biosecurity (Bio) and Cybersecurity (Cyber), collected from GitHub and PubMed, respectively. The retaining set is from Wikitext [42].

**Models.** We need two models to evaluate the performance of unlearning methods: The “origin” model is the starting point of the unlearning process and serves as the performance ceiling for retention. The “retrain” model denotes the golden baseline and provides an upper-bound reference for forgetting.

- **MUSE.** It adopts ICLM-7B [59] and Llama-2-7B as “retrain” models for the BOOKS and NEWS, respectively. Since neither of their pre-training corpora includes MUSE datasets, they can be approximately considered equivalent to retrained. These models are then fine-tuned on MUSE datasets to obtain “origin” models, which are released on Hugging Face.
- **WMDP.** It adopts Zephyr-7B-Beta as the “origin” model, and we extend to modern models, such as Llama-3.1-8B and Qwen3-8B. Notably, a “retrain” model is unavailable due to the widespread distribution of hazardous knowledge across training corpora.

**Metrics.** Different benchmarks design their own metrics based on the unique characteristics of datasets. These metrics can be broadly classified into two categories: *forgetting quality* (FQ) and *retaining utility* (RU). Due to the space limitation, we defer the formal definition of these metrics to [Section B.1](#).

Table 1: The comprehensive unlearning performance comparison between ours and baselines on MUSE, evaluating the forgetting quality and retaining utility from multiple dimensions. KRD represents the overall effectiveness of forgetting, and KnowMem in  $\mathcal{D}_r$  reflects the retention performance. The best results in Forgetting Quality and Retaining Utility are highlighted in **bold**, and the suboptimal ones are marked with an underline.

| Unlearning Method | Forgetting Quality                    |                                       |                             |                        | Retaining Utility                   | Forgetting Quality                    |                                       |                             |                        | Retaining Utility                   |
|-------------------|---------------------------------------|---------------------------------------|-----------------------------|------------------------|-------------------------------------|---------------------------------------|---------------------------------------|-----------------------------|------------------------|-------------------------------------|
|                   | VerbMem<br>$\mathcal{D}_f \downarrow$ | KnowMem<br>$\mathcal{D}_f \downarrow$ | PrivLeak<br>$\rightarrow 0$ | KRD<br>$\rightarrow 1$ | KnowMem<br>$\mathcal{D}_r \uparrow$ | VerbMem<br>$\mathcal{D}_f \downarrow$ | KnowMem<br>$\mathcal{D}_f \downarrow$ | PrivLeak<br>$\rightarrow 0$ | KRD<br>$\rightarrow 1$ | KnowMem<br>$\mathcal{D}_r \uparrow$ |
|                   | <b>BOOKS</b>                          |                                       |                             |                        |                                     | <b>NEWS</b>                           |                                       |                             |                        |                                     |
| Origin            | 99.59                                 | 58.76                                 | 56.68                       | 0.0000                 | 67.00                               | 58.42                                 | 63.41                                 | 99.84                       | 0.0000                 | 54.96                               |
| Retrain           | 14.35                                 | 28.90                                 | 0.00                        | 1.0000                 | 74.38                               | 20.80                                 | 33.30                                 | 0.00                        | 1.0000                 | 54.68                               |
| GA                | 11.00                                 | 23.96                                 | 40.50                       | 0.5452                 | 34.24                               | 4.95                                  | 31.08                                 | 108.10                      | 0.0002                 | 27.33                               |
| NPO               | 20.13                                 | 27.68                                 | 41.35                       | 0.5200                 | 44.75                               | 7.60                                  | 54.62                                 | 105.79                      | 0.0003                 | 41.27                               |
| WHP               | 19.04                                 | 51.49                                 | 51.56                       | 0.1849                 | <b>63.47</b>                        | 17.15                                 | 23.17                                 | 97.56                       | 0.0658                 | 29.90                               |
| SimNPO            | 0.00                                  | 3.24                                  | 17.15                       | <u>0.8737</u>          | 49.55                               | 13.21                                 | 47.82                                 | 11.75                       | <u>0.7380</u>          | 40.66                               |
| RMU               | 7.04                                  | 30.92                                 | 20.45                       | <u>0.8248</u>          | 58.37                               | 18.14                                 | 32.31                                 | 93.77                       | <u>0.1627</u>          | 38.95                               |
| <b>KUDA</b>       | 0.05                                  | 26.73                                 | 16.55                       | <b>0.8792</b>          | <u>61.97</u>                        | 8.71                                  | 0.26                                  | 20.09                       | <b>0.9523</b>          | <b>53.08</b>                        |

- **MUSE.** For *FQ*, MUSE designs three metrics (*VerbMem*, *KnowMem* on  $\mathcal{D}_f$ , and *PrivLeak*). The first two metrics reflect the ability to reproduce training data and to answer questions related to forgetting knowledge. When values are lower than those of the “retrain” model, forgetting is considered completed. Besides, a value closer to 0 is preferred for *PrivLeak*, reflecting good defense against membership inference attacks (MIA). Regarding *RU*, MUSE utilizes *KnowMem* on  $\mathcal{D}_r$ , and the value closer to the “origin” model indicates better retention.
- **WMDP.** It evaluates *FQ* with *Answer Acc* (*Acc*) on multi-choice test sets. 25% is the ideal result, indicating that the model lacks cognition of dangerous knowledge and thus answers at random. Besides, WMDP adopts *MMLU* [21], a multi-domain benchmark covering STEM and humanities, among other disciplines, to assess *RU* of broad world knowledge. The score closer to that of the “origin” model reflects better retention of general knowledge.

The evaluation for *RU* is straightforward, while the metrics for *FQ* are multi-dimensional. Therefore, we propose *knowledge removal degree* (*KRD*), a harmonic mean of forgetting metrics, to quantify the *overall* forgetting performance. When any metric indicates poor forgetting, *KRD* tends towards 0; otherwise, it approaches 1:

$$\text{KRD} = \frac{n}{\sum_{i=1}^n \frac{1}{FQ_i}}, \quad (11)$$

where  $FQ_i$  is the specific metric to assess forgetting in different benchmarks, such as *VerbMem* in MUSE, and is adjusted to eliminate the disruption of over-forgetting. We detail the adjustment process in Section B.1.

**Competitors.** We compare with a series of representative methods: GA [27], NPO [78], SimNPO [14], and the SOTA

method RMU [32]. All methods are implemented with Grad-Diff (GD) [74]. For other baselines, we conduct WHP [12] in MUSE. See Section B.2 for more implementation details.

## 5.2 Overall Unlearning Performance

We evaluate KUDA on MUSE and WMDP, and quantify unlearning performance in terms of forgetting quality and retaining utility.

**Performance on MUSE.** Table 1 presents the results on MUSE. In general, KUDA demonstrates outstanding effectiveness of knowledge removal in both BOOKS and NEWS. The optimal *KRD* values indicate the comprehensive forgetting capabilities, ranging from the deletion of verbatim memorization to privacy protection. Concretely, KUDA significantly reduces both *VerbMem* and *KnowMem* on  $\mathcal{D}_f$  below those of the “retrain” model, suggesting that the LLM’s capacity to utilize the target forgetting knowledge for text generation has been effectively suppressed. In contrast, WHP, NPO, and SimNPO only weaken the model’s ability to reproduce specific training text, reflecting superficial forgetting. Besides, it can be observed that KUDA also shows great improvement in *PrivLeak*, only slightly underperforming SimNPO in NEWS. This reveals that the model unlearned by KUDA can effectively defend against MIA, demonstrating solid capabilities of privacy protection.

Furthermore, KUDA achieves a great balance between forgetting effectiveness and model utility retention. In NEWS, KUDA minimizes degradation in retaining utility while achieving maximal knowledge removal. In BOOKS, although slightly weaker than WHP in retention, KUDA presents significant forgetting effectiveness, indicating a more balanced unlearning performance; In comparison, WHP yields a model with a state close to “not forgetting.” Notably, GA thoroughly removes target knowledge via over-forgetting [58], but at

Table 2: The unlearning performance comparison between ours and baselines on WMDP. Acc-Bio and Acc-Cyber denote the answer accuracy on different test sets. Acc-Avg denotes the weighted average accuracy, with the weights determined by the number of questions in each set. Other definitions are consistent with those of Table 1.

| Method                | Forgetting Quality |            |          | Retaining Utility |              |
|-----------------------|--------------------|------------|----------|-------------------|--------------|
|                       | Acc-Bio↓           | Acc-Cyber↓ | Acc-Avg↓ | KRD→1             | MMLU↑        |
| <b>Zephyr-7B-Beta</b> |                    |            |          |                   |              |
| Origin                | 63.82              | 43.78      | 51.60    | 0.0000            | 58.13        |
| GA                    | 27.06              | 26.82      | 26.92    | <b>0.9244</b>     | 33.02        |
| NPO                   | 42.93              | 36.34      | 38.91    | 0.6813            | 45.71        |
| SimNPO                | 39.61              | 33.79      | 36.06    | 0.5741            | 48.26        |
| RMU                   | 29.22              | 27.93      | 28.43    | 0.8665            | 56.90        |
| <b>KUDA</b>           | 29.92              | 26.82      | 28.03    | <b>0.8879</b>     | <b>57.14</b> |
| <b>Llama-3.1-8B</b>   |                    |            |          |                   |              |
| Origin                | 59.62              | 41.87      | 48.80    | 0.0000            | 63.31        |
| RMU                   | 30.00              | 26.27      | 27.73    | 0.8888            | 58.33        |
| <b>KUDA</b>           | 29.22              | 25.00      | 26.28    | <b>0.9350</b>     | <b>60.64</b> |
| <b>Qwen-3-8B</b>      |                    |            |          |                   |              |
| Origin                | 74.16              | 45.14      | 56.47    | 0.0000            | 73.01        |
| RMU                   | 36.52              | 34.35      | 35.30    | 0.6304            | 60.02        |
| <b>KUDA</b>           | 28.43              | 26.17      | 27.05    | <b>0.9360</b>     | <b>68.92</b> |

the cost of severely compromising model utility and even increasing vulnerability to MIA. From the perspective, KUDA reveals that its unlearning mechanism dives into knowledge encoded in LLMs, without excessive destruction to model utility.

Moreover, RMU presents strong performance in both forgetting and retention. However, KUDA excels further in dataset generalization, comprehensive knowledge removal, and utility preservation.

**Performance on WMDP.** In Table 2, we present the performances on WMDP. In general, KUDA achieves both effective forgetting and strong utility retention. It removes 88.8% hazardous knowledge stored in Zephyr-7B-Beta, with only a negligible 1.3% drop in retaining utility. Notably, it maintains better performance than RMU, even though RMU is the SOTA method on this benchmark. As for other baselines, GA leads to severe degradation in retaining utility for achieving forgetting. NPO and its variant SimNPO struggle to eliminate the LLM’s ability to utilize dangerous knowledge, as observed in the experiments of MUSE. Fan *et al.* [14] attribute this to the primary focus of NPO on aligning text-level responses, instead of the knowledge encoded in parameters. In contrast, KUDA achieves multi-dimensional unlearning.

Furthermore, since the “origin” model for WMDP does not require dataset-specific fine-tuning, we extend our experiments to more modern architectures, Llama-3.1 and Qwen-3. In subsequent experiments, we only compare with RMU, as

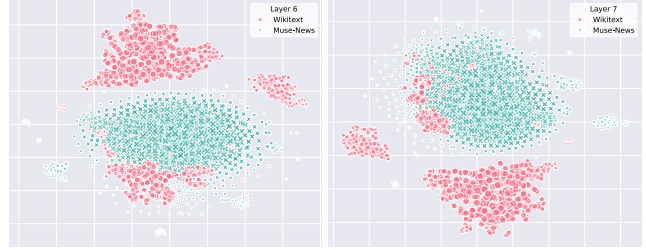


Figure 3: t-SNE visualization of representations on Wikitext and MUSE-News.

both KUDA and RMU substantially outperform all other baselines.

Overall, KUDA consistently surpasses RMU, particularly on Qwen-3. Both the Zephyr and Llama series originate from the Llama architecture family, sharing high similarity in model design and compatibility. In contrast, Qwen-3 incorporates architectural innovations such as QK-Norm and a deeper stack of layers. We attribute RMU’s limited transferability primarily to poor compatibility to these architectural differences. Therefore, this demonstrates the robust model generalization capability of KUDA.

**Retention Transferability.** We further observe that KUDA mitigates the reliance on the knowledge distribution of the retaining set to some extent. It avoids significant degradation in the model’s factual cognition on general knowledge, even when  $\mathcal{D}_r$  is semantically unrelated to them. Concretely, we perform unlearning with domain-specific retaining sets  $\mathcal{D}_r$ , including articles on biology and cybersecurity, Harry Potter-related content, and BBC news. Then we adopt MMLU to assess the unlearned models’ cognition of multi-domain world knowledge.

Across all datasets, KRD scores exceed 0.9, while MMLU scores show only minor degradation: 58.13 → 55.50 (Zephyr-7B-Beta), 36.81 → 36.23 (MUSE-NEWS “origin” model), and 26.52 → 25.97 (MUSE-BOOKS “origin” model). The t-SNE analysis in Figure 3 reveals the inseparability between the representations of these domain-specific knowledge instances and those from Wikitext, which covers general-domain knowledge. Therefore, when KUDA applies null-space to mitigate the adverse impact on the representations of domain-specific retaining knowledge, it inadvertently preserves the representations of multi-domain general knowledge.

### 5.3 Mechanism Analysis

We aim to investigate the underlying reasons why KUDA achieves a better balance between knowledge removal and utility retention than other unlearning baselines. Therefore, we conduct a mechanistic analysis experiment from the perspective of *gradient dynamics*.

Table 3: The unlearning performance on WMDP-Augment using a domain-adjacent but benign  $\mathcal{D}_r$  relative to  $\mathcal{D}_f$ .

| Method      | Forgetting Quality |            |          | Retaining Utility |       |
|-------------|--------------------|------------|----------|-------------------|-------|
|             | Acc-Bio↓           | Acc-Cyber↓ | Acc-Avg↓ | KRD→1             | MMLU↑ |
| RMU         | 33.22              | 26.57      | 29.17    | 0.8475            | 51.85 |
| <b>KUDA</b> | 32.00              | 26.50      | 28.70    | 0.8670            | 54.50 |

**Setup.** Previous studies [66, 70] have identified the optimization challenge in gradient-based unlearning methods: the gradients of  $\mathcal{L}_f$  and  $\mathcal{L}_r$  mutually impede each other during the parameter updates. This highlights the essence of non-conflicting gradients for successful unlearning. Based on the insight, we design an experiment focusing on gradient conflicts to elucidate the unlearning mechanism of KUDA.

We conduct experiments on WMDP and change the original  $\mathcal{D}_r$  Wikitext. With the knowledge independent of cyber- or bio-related hazardous content in  $\mathcal{D}_f$ , Wikitext avoids significant conflicts between forgetting and retention objectives, thereby facilitating a high-quality unlearning balance. To magnify the optimization conflicts, we construct a stringent scenario by using  $\mathcal{D}_r$  that consists of benign knowledge, which is semantically adjacent to  $\mathcal{D}_f$ . We compare with RMU, the SOTA method in WMDP, and tune hyperparameters until the RMU-unlearned and KUDA-unlearned models achieve comparable forgetting quality. To prevent over-forgetting, we ensure that both models achieve scores above 25 on the Bio and Cyber evaluation tests. Throughout training, we record the cosine similarity between the gradients of  $\mathcal{L}_f$  and  $\mathcal{L}_r$ , and convert it to the angular value in degrees for intuitive interpretability.

**Observations.** Table 3 exhibits a comparable forgetting quality, and RMU incurs more severe degradation of model utility. This indicates that KUDA allows more precise and targeted knowledge removal, even when it is removed from semantically proximate or related knowledge domains. Figure 4 shows the evolution of gradient angles, further revealing the underlying mechanism behind the above observations from the perspective of gradient alignment.

The gradient angles of RMU predominantly fall within the range of  $90^\circ \sim 120^\circ$ , particularly in the early and middle phases. This suggests a severe imbalance between conflicting objectives, leading to an increased risk of collapse in model utility. This may stem from the design of RMU’s losses (see introduction in Section 3.2), which employs symmetric MSE for both forgetting and retention, and is thus prone to gradient conflicts.

In contrast, KUDA presents more stable gradient dynamics, with the gradient angles between  $\mathcal{L}_f$  and  $\mathcal{L}_r$  fluctuating around  $90^\circ$ . This illustrates that KUDA, as a gradient-based method, inherently maintains near-orthogonal alignment between forgetting and retaining gradients during unlearning. Therefore, it avoids the dilemma of optimization conflicts

posed by antagonistic interference, thus eliminating the need to compromise the model utility for knowledge removal. We attribute this advantage to the synergy effect of well-designed unlearning losses and relaxation null-space projection.

## 5.4 Hyperparameter Analysis

We further evaluate the impact of two critical hyperparameters and support our guidance for hyperparameter search.

**Setup.** We adopt WMDP for hyperparameter analysis due to the well-curated data scale and evaluation efficiency, which enable rapid iteration over variant configurations. We vary inverse unlearning temperature  $\beta$  over a set of  $\{0.1, 1.0, 2.0\}$ , sample five values for null-space relaxation threshold  $\tau$  from the range  $3 \times 10^{-4} \sim 3 \times 10^{-3}$ , and then conduct a cross-combination study over these hyperparameters. Preliminary experiments are deferred to Section C.2.

**Impact of Inverse Unlearning Temperature  $\beta$ .** Figure 5 presents a heatmap of the hyperparameter experiment results, where darker shades denote better performance. It can be observed that the choice of  $\beta$  significantly affects the unlearning performance: smaller values of  $\beta$  lead to stronger knowledge removal but at the cost of degrading the model utility retention. Moreover, the impact of  $\beta$  on forgetting exhibits a similar tendency across different values of  $\tau$ .

These results correspond to our method, where  $\beta$  controls the step size of the forgetting process. In general, as  $\beta$  increases, the divergence degree gradually weakens. This leads to a gradual reduction in the intensity of knowledge removal, with the unlearned model tending toward a state of “weak forgetting.” Correspondingly, the retaining utility improves progressively, approaching that of the “origin” model.

**Impact of Null-Space Relaxation Threshold  $\tau$ .** As shown in Figure 5, decreasing  $\tau$  significantly enhances retaining utility while gradually weakening forgetting effectiveness. Notably, the retaining utility is sensitive to variations in  $\beta$  under a large  $\tau$ ; however, this sensitivity declines and turns to robustness against  $\beta$  variations once  $\tau$  drops below a certain value. We identify the specific  $\tau$  as “stability boundary”, at or below which the forgetting process is significantly suppressed, as presented in Figure 9 of Section C.2.

The observed trend aligns with our predictions, confirming that  $\tau$  influences the trade-off between forgetting and retention. Specifically,  $\tau$  dictates the singular value filtering range, thus controlling the selection of singular vectors used to construct the approximate null-space. Lower values of  $\tau$  mean fewer singular vectors, which typically correspond to feature directions with minimal contribution to the representation space. Therefore, the null-space becomes weakly correlated with the representations of retaining knowledge. Due to the entanglement discussed in Section 4.5, projecting gradients into this subspace limits perturbation to retaining knowledge, while it also constrains knowledge removal. The interaction

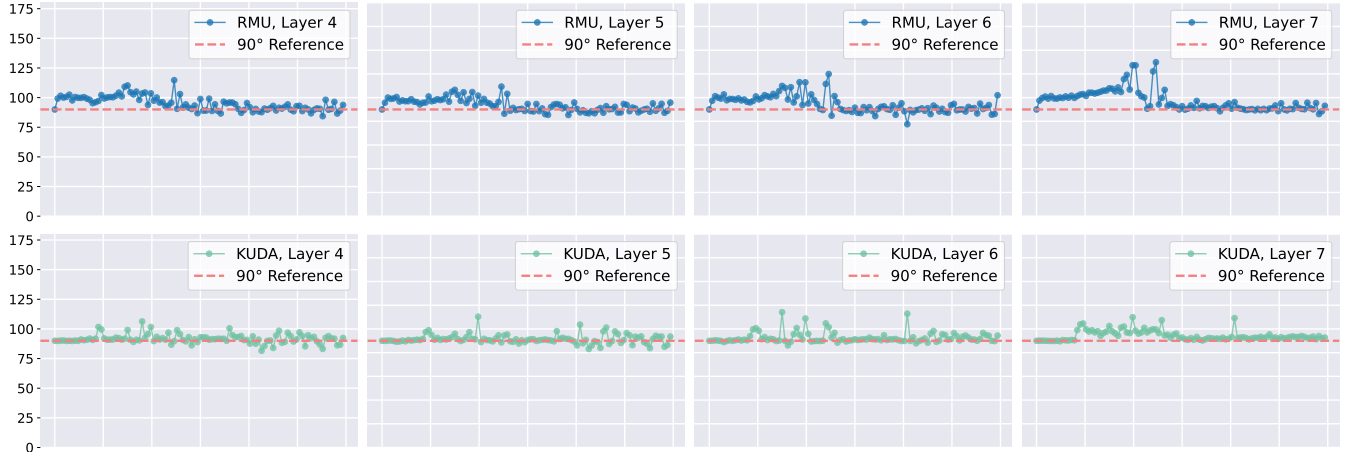


Figure 4: Evolution of angles between two gradients during the unlearning with RMU and KUDA. We trained on WMDP for 600 steps, showcasing the gradient angle fluctuations throughout the entire process.

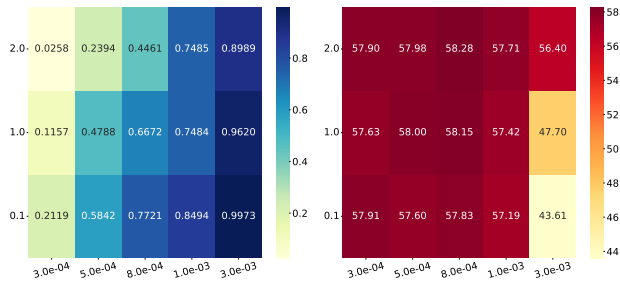


Figure 5: Unlearning performance heatmap across different hyperparameter combinations of  $\beta$  (vertical axis) and  $\tau$  (horizontal axis). The left plot presents forgetting quality with KR D, and the right one shows retaining utility via MMLU score. Darker colors indicate better performance.

explains why  $\tau$  affects KUDA’s sensitivity to the changes of  $\beta$ .

**Summary.** Based on the comprehensive analysis, we identify the observations: (1) Decreasing  $\beta$  strengthens the forgetting intensity and leads to more aggressive removal of target knowledge; (2) Decreasing  $\tau$  improves retaining utility with the cost of reduced forgetting effectiveness; (3) Knowledge removal is suppressed if  $\tau$  is at or below the stability boundary. (4) When  $\tau$  falls below stability boundary, changes in  $\beta$  yield limited influence on retention.

These observations reveal the coupled impact of  $\beta$  and  $\tau$ , where both hyperparameters concurrently modulate the trade-off between knowledge removal and utility retention. Beyond their direct influence on unlearning,  $\tau$  further regulates the impact from variations of  $\beta$ . This interdependence highlights the necessity of our two-stage tuning strategy that simplifies the complex joint optimization into two decoupled linear processes. Moreover, Observation (3) refines the strategy that



Figure 6: Unlearning performance across different unlearning layers. The horizontal axis shows the unlearning layers.  $i \sim j$  denotes that all layers from  $i$  to  $j$  are designated as unlearning layers, and “w/o  $k$ ” means the excluded layer  $k$ .

$\tau$  should moderately increase if adjusting  $\beta$  yields a negligible impact.

## 5.5 Ablation Study

We also conduct ablation experiments to verify the effectiveness of KUDA’s components.

**Effectiveness of Layer Selection.** We set five baselines to validate layer selection: (1) Depth-based layers comprising Shallow ( $l_3 \sim l_6$ ), Middle ( $l_{12} \sim l_{15}$ ), and Deep ( $l_{21} \sim l_{24}$ ) layers; and (2) Functional partitions, focusing on the FFN-dominant ( $l_3 \sim l_9$ ) and MHSA-dominant ( $l_{15} \sim l_{18}$ ) zones as shown in Figure 7.

Figure 6 demonstrates that KUDA is position-sensitive to the unlearning layers, with randomized selections at various layer depths for comparison. Particularly, although the middle and deep layers aggregate knowledge via residual streams, they fail to effectively remove knowledge. Besides, our layer selection strategy achieves a functional decoupling between

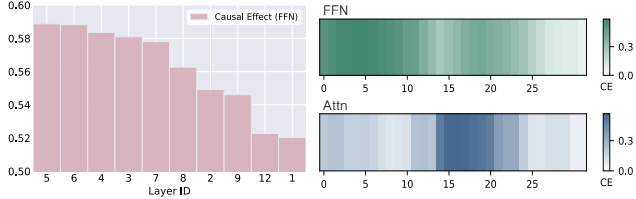


Figure 7: Visualization of causal effect on Zephyr-7B-Beta. The left plot presents the layers with Top-10 causal effect in FFN components. The right panels present the global causal effects, with darker colors indicating stronger causal effects.

Table 4: The forgetting quality and retaining utility of unlearned models with different loss functions ( $\mathcal{L}_{\text{RMU}}$  and  $\mathcal{L}_{\text{KUDA}}$ ), GradDiff (GD), and Null-Space Projection (NSP). WMDP-Augment uses adjacent, benign knowledge as  $\mathcal{D}_r$ .

| Dataset      | Method                            | Forgetting Quality ↓ | Retaining Utility ↑ |
|--------------|-----------------------------------|----------------------|---------------------|
| WMDP-Augment | $\mathcal{L}_{\text{RMU}}$ + GD   | 28.17                | 51.85               |
|              | $\mathcal{L}_{\text{RMU}}$ + NSP  | 27.45                | 51.22               |
|              | $\mathcal{L}_{\text{KUDA}}$ + GD  | 28.60                | 52.48               |
|              | $\mathcal{L}_{\text{KUDA}}$ + NSP | 27.40                | 55.50               |
| MUSE-BOOKS   | $\mathcal{L}_{\text{RMU}}$ + GD   | 30.92                | 58.37               |
|              | $\mathcal{L}_{\text{RMU}}$ + NSP  | 34.58                | 53.60               |
|              | $\mathcal{L}_{\text{KUDA}}$ + GD  | 31.67                | 55.95               |
|              | $\mathcal{L}_{\text{KUDA}}$ + NSP | 32.48                | 63.11               |

the FFN-dominant zone and the MHSA-dominant zone, as presented Figure 7. The results in Figure 6 indicate that this decoupling enables knowledge removal without compromising the models’ core utility. Notably, we observe a robust layer selection interval ( $I_4 \sim I_9$ ) that consistently yields superior performance, with minor trade-off fluctuations between forgetting and retention. All layers within the interval have high  $\text{CE}_{\text{FFN}}$ , and layers identified by our strategy also reside in.

**Effectiveness of Knowledge Representation Deviation Loss.** To verify the necessity of the KUDA loss, we substitute it with  $\mathcal{L}_{\text{RMU}}$  and compare the retaining utility at a comparable level of forgetting quality. To simplify the analysis, we adopt average weighted answer accuracy and MMLU scores on WMDP, along with KnowMem in  $\mathcal{D}_f$  and  $\mathcal{D}_r$  on MUSE, as intuitive metrics to quantify forgetting quality and retaining utility, respectively.

Table 4 indicates the better compatibility between  $\mathcal{L}_{\text{KUDA}}$  and null-space projection than  $\mathcal{L}_{\text{RMU}}$ , with their synergy effectively improving both knowledge removal and utility retention. This suggests that the asymmetric design of  $\mathcal{L}_{\text{KUDA}}$  serves as a fundamental prerequisite that allows relaxation null-space projection to retain model utility without hindering knowledge removal.

**Effectiveness of Null-space Projection.** Given that null-space projection serves as an enhancement to GradDiff, we

Table 5: The time cost in HH:MM:SS format, with 4 unlearning layers. The cost of parameter update denotes one epoch, and the update without projection is also reported.

| Dataset | Model          | Causal Tracing | Input Feature | SVD     | Update  | Update w/o Projection |
|---------|----------------|----------------|---------------|---------|---------|-----------------------|
|         | Zephyr-7B-Beta | 2:10:23        | 0:02:40       | 0:09:40 | 0:05:57 | 0:04:28               |
| WMDP    | Llama-3.1-8B   | 2:57:00        | 0:04:16       | 0:09:33 | 0:08:21 | 0:06:25               |
|         | Qwen3-8B       | 2:41:45        | 0:02:32       | 0:18:32 | 0:08:17 | 0:06:34               |
| BOOKS   | ICLM-7B        | 2:21:06        | 0:00:32       | 0:04:08 | 0:12:23 | 0:11:18               |
| NEWS    | Llama-2-7B     | 1:50:24        | 0:03:04       | 0:04:12 | 0:09:05 | 0:08:25               |

adopted it for comparison. The baseline unlearning loss is formulated as  $\mathcal{L}_u = \mathcal{L}_f + \alpha \cdot \mathcal{L}_r$ , where  $\alpha$  is the scaling factor. Other settings are consistent with those described in the above part.

Table 4 demonstrates that, under the loss of KUDA, null-space projection outperforms GradDiff in balancing the forgetting and retention, consistently across different datasets and models. Particularly, at comparable forgetting quality, null-space projection significantly improves retention performance. We attribute this to its ability to alleviate optimization conflicts through subspace transformations, rather than merely adjusting the relative magnitudes of gradients with a scaling factor. Therefore, it eliminates the adverse influence of the update gradients on the representation space of retaining knowledge.

## 5.6 Efficiency Analysis

**Computational Overhead.** Table 5 presents the computational overhead of KUDA, identifying “causal tracing” as the primary bottleneck. However, as discussed in Section 4.3, this phase is a one-time offline operation for each model, with the selected unlearning layers being reusable across various datasets. The computational cost of SVD is primarily determined by the dimensionality of the input features, but remains acceptable when restricted to a few unlearning layers. Moreover, the additional overhead introduced by the projection during parameter updates is marginal across models and unlearning tasks.

In general, KUDA introduces acceptable additional overhead, which remains stable and does not scale significantly with the size or complexity of the unlearning tasks. However, the computational overhead of “Input Feature Capture” scales linearly with the size of  $\mathcal{D}_r$ , leaving an issue we address specifically in the following.

**Sample Strategy.** To mitigate the computational bottleneck caused by “Input Feature Capture” under a large-scale dataset, we propose stochastic proportional sampling in Section 4.5 to construct an approximate input feature space using a sampled

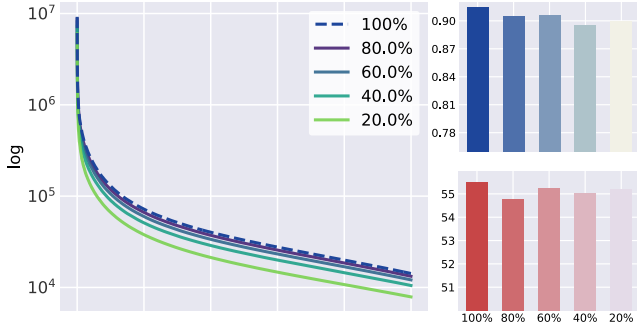


Figure 8: Impact of sampling ratio. The left plot shows the result of eigendecomposition, in descending order on a logarithmic scale. The right plot presents forgetting quality (top) and retaining utility (bottom), under different sampling ratios and tuning  $\tau$ .

subset  $\hat{\mathcal{D}}_r$ . A critical consideration is whether such a sampling strategy preserves the information integrity of input features, or if it leads to a degradation in the effectiveness of null-space due to potential information loss.

We conduct a comprehensive analysis with different sampling ratios  $p$  and a large-scale corpus with 61,000 samples, following basic unlearning evaluations and spectral decomposition analysis on the input feature spaces. As presented in Figure 8, the high consistency of eigenvalue spectra confirms that stochastic sampling effectively captures the primary information and core distribution of the original representation space. Since relaxation null-space projection primarily targets preserving these dominant features, the inevitable minor information loss only induces variations in the construction of null-space, without compromising its protection function. Figure 8 confirms that near-optimal unlearning performance can be achieved across ratios  $p$  through minor adjustments of  $\tau$ , while reducing the overhead to  $\frac{p}{100}$  of the original one, thus balancing computational efficiency with the unlearning effectiveness.

## 6 Related Work

### 6.1 LLM Unlearning

LLM unlearning is an extension of machine unlearning [2–5] that is specifically applied to LLMs, to remove undesired knowledge from a pre-trained LLM without full retraining [36, 52]. Representative methods for LLM unlearning primarily rely on *parameter modifications*. This includes full parameter updates based on specific forgetting losses [14, 27, 78], which often incorporate retaining losses to balance forgetting and retention [74], serving as the foundational approach. To pursue higher efficiency and balance, some studies focus on identifying parameters correlated to target knowledge [30, 46, 72]. However, these are computationally

expensive, restricting practical applicability. Besides, researchers explore partial parameter updates based on activations steering [32, 55], but the effectiveness of forgetting is limited [13, 73].

In contrast to parameter modifications, the *external intervention* methods introduce external components to interfere with the generation process, such as context fine-tuning [59], or by adding perturbations to input embeddings [35] or output logits [29]. Therefore, these methods control the model to exhibit “unlearning” behavior without updating the model parameters. However, these only achieve unlearning at the behavioral level, failing to remove the target knowledge encoded within the model’s parameters. This renders such methods vulnerable to the risk of target knowledge being extracted from the model’s intermediate representations [62]. These approaches are excluded from our discussion and evaluation because they do not fulfill the fundamental requirement of LLM unlearning, specifically the removal of targeted knowledge. Therefore, they are considered distinct from the scope of our research.

### 6.2 LLM Unlearning Verification

The validation of unlearning effectiveness deserves attention, as it is not only essential for providing a unified evaluation framework but also a critical step toward enabling the practical deployment of unlearning. A central criterion is to construct a golden baseline model as a reference, which approximates retraining on the retaining dataset [52]. Benchmarks such as TOFU [39] and MUSE [58] build forgetting sets from corpora published after the release of specific models. These models serve as golden baselines, as they have no exposure to the forgetting set, while models fine-tuned on the datasets are treated as the starting point of unlearning models. WMDP [32] constructs a multi-choice question set centered on hazardous knowledge and establishes a human-defined criterion as the ideal performance of a golden baseline. Additionally, it utilizes MMLU [21] to evaluate the LLMs’ retention of general knowledge. Regarding evaluation metrics, researchers focus on the balance between forgetting quality and retaining utility, often assessed by the form of question-answering [32, 39, 58].

### 6.3 Attacks against LLM Unlearning

The robustness of an unlearned LLM against adversarial attacks is also a critical aspect for ensuring practical applicability [36]. On one hand, existing attacks aim to extract forgotten knowledge by exploiting residual memory through adversarial attacks [79] or backdoor triggers [26]. On the other hand, the adversary recovers the forgotten knowledge through specific prompts [77] that simply emphasize certain keywords in the prompts. Notably, even without access to the forgetting set, the supposedly removed information can be restored by fine-tuning on retaining sets [24] or even on unrelated down-

stream tasks [64]. These reveal the vulnerability of existing knowledge-removal-intended methods, indicating that they tend to obscure knowledge rather than remove it [52].

## 6.4 Application of LLM Unlearning

Explorations across diverse application domains have revealed a broad potential of LLM unlearning, including the removal of privacy-sensitive training data encoded in LLMs [7, 27, 72], the suppression of harmful content generation [32, 37], and the enforcement of copyright compliance [9]. Furthermore, related research has extended its scope to address training data contamination, encompassing issues such as noisy data [65], mislabeled content [60], and backdoor attacks [23, 31, 54, 61, 80].

## 6.5 Model Editing

Model editing aims to modify the knowledge of pre-trained LLMs by redirecting specific inputs to targeted outputs [69, 75], and the “Locate-and-Edit” has emerged as a mainstream paradigm [69]. The representative method, ROME [40], locates FFNs as knowledge storage and applies a rank-1 update to modify knowledge. Subsequent works include MEMIT [41], PMET [33], EMMET [19], and AlphaEdit [15]. Despite sharing the same technical intuition of localized parameter updates, our method is distinct from model editing. Model editing essentially redirects knowledge mappings to the given outputs, while LLM unlearning focuses on removing such mappings. This lack of substitute targets makes LLM unlearning confronted with severe utility degradation, and hinders the direct migration of editing algorithms. Besides, model editing typically targets atomic factual triples (Subject, Relation, Object) with relative locality. LLM unlearning, however, addresses broader concepts or data traces that lead to significant knowledge entanglement.

## 7 Conclusion

In this paper, we focus on the LLMs’ property of knowledge storage for effective unlearning. We propose KUDA, a representation-based method that enables targeted parameter updates for knowledge removal with minimal degradation on model utility. KUDA utilizes a component-level identification method with a sliding window strategy to select unlearning layers, introduces a representation deviation mechanism to remove target knowledge, and employs the relaxation null-space projection to preserve the representations of retaining knowledge. Besides, we propose a two-stage tuning strategy to decouple the complex joint hyperparameter searches. Experimental results demonstrate that KUDA outperforms most representative baselines in balancing both knowledge removal and utility retention, and we further reveal the underlying mechanism.

## References

- [1] Maksym Andriushchenko, Francesco Croce, and Nicolas Flammarion. Jailbreaking Leading Safety-Aligned LLMs with Simple Adaptive Attacks. In *ICLR*, 2025.
- [2] Lucas Bourtole, Varun Chandrasekaran, Christopher A. Choquette-Choo, Hengrui Jia, Adelin Travers, Baiwu Zhang, David Lie, and Nicolas Papernot. Machine Unlearning. In *S&P*, pages 141–159, 2021.
- [3] Huiqiang Chen, Tianqing Zhu, Xin Yu, and Wanlei Zhou. Machine unlearning via null space calibration. In *IJCAI*, pages 358–366, 2024.
- [4] Min Chen, Zhikun Zhang, Tianhao Wang, Michael Backes, Mathias Humbert, and Yang Zhang. When machine unlearning jeopardizes privacy. In *CCS*, pages 896–911, 2021.
- [5] Min Chen, Zhikun Zhang, Tianhao Wang, Michael Backes, Mathias Humbert, and Yang Zhang. Graph unlearning. In *CCS*, pages 499–513, 2022.
- [6] Min Chen, Zhikun Zhang, Tianhao Wang, Michael Backes, and Yang Zhang. FACE-AUDITOR: Data Auditing in Facial Recognition Systems. In *USENIX Security*, 2023.
- [7] Zhaoyang Chu, Yao Wan, Zhikun Zhang, Di Wang, Zhou Yang, Hongyu Zhang, Pan Zhang, Xuanhua Shi, Hai Jin, and David Lo. Scrub It Out! Erasing Sensitive Memorization in Code Language Models via Machine Unlearning. In *ICSE*, 2026.
- [8] Cortes, Corinna and Mohri, Mehryar and Rostamizadeh, Afshin. L2 Regularization for Learning Kernels. In *UAI*, page 109–116, 2009.
- [9] Guangyao Dou, Zheyuan Liu, Qing Lyu, Kaize Ding, and Eric Wong. Avoiding Copyright Infringement via Large Language Model Unlearning. In *NAACL*, pages 5176–5200, 2025.
- [10] Linkang Du, Xuanru Zhou, Min Chen, Chusong Zhang, Zhou Su, Peng Cheng, Jiming Chen, and Zhikun Zhang. Sok: Dataset Copyright Auditing in Machine Learning Systems. In *S&P*, pages 1–19, 2025.
- [11] Yanai Elazar, Shauli Ravfogel, Alon Jacovi, and Yoav Goldberg. Amnesic Probing: Behavioral Explanation with Amnesic Counterfactuals. *Transactions of the Association for Computational Linguistics*, pages 160–175, 2021.
- [12] Ronen Eldan and Mark Russinovich. Who’s Harry Potter? Approximate Unlearning in LLMs. *arXiv preprint*, 2023.
- [13] Chongyu Fan, Jinghan Jia, Yihua Zhang, Anil Ramakrishna, Mingyi Hong, and Sijia Liu. Towards LLM Unlearning Resilient to Relearning Attacks: A Sharpness-Aware Minimization Perspective and Beyond. In *ICML*, 2025.
- [14] Chongyu Fan, Jiancheng Liu, Licong Lin, Jinghan Jia, Ruiqi Zhang, Song Mei, and Sijia Liu. Simplicity Prevails: Rethinking Negative Preference Optimization for LLM Unlearning. In *NeurIPS Safe Generative AI Workshop*, 2024.
- [15] Junfeng Fang, Houcheng Jiang, Kun Wang, Yunshan Ma, Jie Shi, Xiang Wang, Xiangnan He, and Tat-Seng Chua. AlphaEdit: Null-Space Constrained Knowledge Editing for Language Models. In *ICLR*, 2025.
- [16] Javier Ferrando, Gerard I Gállego, Ioannis Tsiamas, and Marta R Costa-jussà. Explaining How Transformers Use Context to Build Predictions. In *ACL*, pages 5486–5513, 2023.
- [17] Mor Geva, Jasmijn Bastings, Katja Filippova, and Amir Globerson. Dissecting Recall of Factual Associations in Auto-Regressive Language Models. In *EMNLP*, pages 12216–12235, 2023.
- [18] Mor Geva, Roei Schuster, Jonathan Berant, and Omer Levy. Transformer feed-forward layers are key-value memories. In *EMNLP*, pages 5484–5495, 2021.
- [19] Akshat Gupta, Dev Sajani, and Gopala Anumanchipalli. A Unified Framework for Model Editing. In *Findings of EMNLP*, pages 15403–15418, 2024.
- [20] Michael Hanna, Ollie Liu, and Alexandre Variengien. How Does GPT-2 Compute Greater-Than?: Interpreting Mathematical Abilities in a Pre-trained Language Model. In *NeurIPS*, pages 76033–76060, 2023.
- [21] Dan Hendrycks, Collin Burns, Steven Basart, Andy Zou, Mantas Mazeika, Dawn Song, and Jacob Steinhardt. Measuring Massive Multitask Language Understanding. In *ICLR*, 2021.
- [22] Yihuai Hong, Yuelin Zou, Lijie Hu, Ziqian Zeng, Di Wang, and Haiqin Yang. Dissecting Fine-Tuning Unlearning in Large Language Models. In *EMNLP*, pages 3933–3941, 2024.
- [23] Man Hu, Yahui Ding, Yatao Yang, Liangyu Chen, Yanhao Jia, and Shuai Zhao. DUP: Detection-guided Unlearning for Backdoor Purification in Language Models. *arXiv preprint*, 2025.
- [24] Shengyuan Hu, Yiwei Fu, Steven Wu, and Virginia Smith. Jogging the Memory of Unlearned Models through Targeted Relearning Attacks. In *ICML Workshop on Foundation Models in the Wild*, 2024.

- [25] Yue Huang, Lichao Sun, Haoran Wang, Siyuan Wu, Qihui Zhang, Yuan Li, Chuji Gao, Yixin Huang, Wenhan Lyu, Yixuan Zhang, et al. Position: TrustLLM: Trustworthiness in Large Language Models. In *ICML*, 2024.
- [26] Dang Huu-Tien, Hoang Thanh-Tung, Anh Bui, Le-Minh Nguyen, and Naoya Inoue. Improving LLM Unlearning Robustness via Random Perturbations. *arXiv preprint*, 2025.
- [27] Joel Jang, Dongkeun Yoon, Sohee Yang, Sungmin Cha, Moontae Lee, Lajanugen Logeswaran, and Minjoon Seo. Knowledge Unlearning for Mitigating Privacy Risks in Language Models. In *ACL*, pages 14389–14408.
- [28] Ganesh Jawahar, Benoît Sagot, and Djamel Seddah. What does BERT Learn about the Structure of Language? In *ACL*, pages 3651–3657, 2019.
- [29] Jiabao Ji, Yujian Liu, Yang Zhang, Gaowen Liu, Ramana Rao Kompella, Sijia Liu, and Shiyu Chang. Reversing the Forget-Retain Objectives: An Efficient LLM Unlearning Framework from Logit Difference. In *NeurIPS*, pages 12581 – 12611, 2025.
- [30] Jinghan Jia, Jiancheng Liu, Yihua Zhang, Parikshit Ram, Nathalie Baracaldo, and Sijia Liu. WAGLE: Strategic Weight Attribution for Effective and Modular Unlearning in Large Language Models. In *NeurIPS*, pages 55620 – 55646, 2024.
- [31] Peihai Jiang, Xixiang Lyu, Yige Li, and Jing Ma. Backdoor Token Unlearning: Exposing and Defending Backdoors in Pretrained Language Models. In *AAAI*, pages 24285–24293, 2025.
- [32] Nathaniel Li, Alexander Pan, Anjali Gopal, Summer Yue, Daniel Berrios, Alice Gatti, Justin D Li, Ann-Kathrin Dombrowski, Shashwat Goel, Long Phan, et al. The WMDP Benchmark: Measuring and Reducing Malicious Use with Unlearning. In *ICML*, 2024.
- [33] Xiaopeng Li, Shasha Li, Shezheng Song, Jing Yang, Jun Ma, and Jie Yu. Pmet: Precise model editing in a transformer. In *AAAI*, pages 18564–18572, 2024.
- [34] Yinheng Li, Shaofei Wang, Han Ding, and Hang Chen. Large Language Models in Finance: A Survey. In *ICAIF*, pages 374–382, 2023.
- [35] Chris Yuhao Liu, Yaxuan Wang, Jeffrey Flanigan, and Yang Liu. Large Language Model Unlearning via Embedding-Corrupted Prompts. In *NeurIPS*, pages 118198 – 118266, 2024.
- [36] Sijia Liu, Yuanshun Yao, Jinghan Jia, Stephen Casper, Nathalie Baracaldo, Peter Hase, Yuguang Yao, Chris Yuhao Liu, Xiaojun Xu, Hang Li, et al. Rethinking Machine Unlearning for Large Language Models. *Nature Machine Intelligence*, pages 1–14, 2025.
- [37] Weikai Lu, Ziqian Zeng, Jianwei Wang, Zhengdong Lu, Zelin Chen, Huiping Zhuang, and Cen Chen. Eraser: Jailbreaking Defense in Large Language Models via Unlearning Harmful Knowledge. *arXiv preprint*, 2024.
- [38] Ziming Luo, Zonglin Yang, Zexin Xu, Wei Yang, and Xinya Du. LLM4SR: A Survey on Large Language Models for Scientific Research. *arXiv preprint*, 2025.
- [39] Pratyush Maini, Zhili Feng, Avi Schwarzschild, Zachary Chase Lipton, and J Zico Kolter. TOFU: A Task of Fictitious Unlearning for LLMs. In *COLM*, 2024.
- [40] Kevin Meng, David Bau, Alex Andonian, and Yonatan Belinkov. Locating and Editing Factual Associations in GPT. In *NeurIPS*, pages 17359–17372, 2022.
- [41] Kevin Meng, Arnab Sen Sharma, Alex J Andonian, Yonatan Belinkov, and David Bau. Mass-Editing Memory in a Transformer. In *ICLR*, 2023.
- [42] Stephen Merity, Caiming Xiong, James Bradbury, and Richard Socher. Pointer Sentinel Mixture Models. *arXiv preprint*, 2016.
- [43] Maximilian Mozes, Xuanli He, Bennett Kleinberg, and Lewis D. Griffin. Use of LLMs for Illicit Purposes: Threats, Prevention Measures, and Vulnerabilities. *arXiv preprint*, 2023.
- [44] Milad Nasr, Javier Rando, Nicholas Carlini, Jonathan Hayase, Matthew Jagielski, A. Feder Cooper, Daphne Ippolito, Christopher Choquette-Choo, Florian Tramèr, and Katherine Lee. Scalable Extraction of Training Data from Aligned, Production Language Models. In *ICLR*, 2025.
- [45] Long Ouyang, Jeffrey Wu, Xu Jiang, Diogo Almeida, Carroll Wainwright, Pamela Mishkin, Chong Zhang, Sandhini Agarwal, Katarina Slama, Alex Ray, et al. Training Language Models to Follow Instructions with Human Feedback. In *NeurIPS*, pages 27730–27744, 2022.
- [46] Nicholas Pochinkov and Nandi Schoots. Dissecting Language Models: Machine Unlearning via Selective Pruning. *arXiv preprint*, 2024.
- [47] Xiangyu Qi, Ashwinee Panda, Kaifeng Lyu, Xiao Ma, Subhrajit Roy, Ahmad Beirami, Prateek Mittal, and Peter Henderson. Safety Alignment Should be Made More Than Just a Few Tokens Deep. In *ICLR*, 2025.

- [48] Xiangyu Qi, Yi Zeng, Tinghao Xie, Pin-Yu Chen, Ruoxi Jia, Prateek Mittal, and Peter Henderson. Fine-tuning Aligned Language Models Compromises Safety, Even When Users Do Not Intend To! In *ICLR*, 2024.
- [49] Ruichen Qiu, Jiajun Tan, Jiayue Pu, Honglin Wang, Xiao-Shan Gao, and Fei Sun. A Survey on Unlearning in Large Language Models. *arXiv preprint*, 2025.
- [50] Rafael Rafailov, Archit Sharma, Eric Mitchell, Christopher D Manning, Stefano Ermon, and Chelsea Finn. Direct Preference Optimization: Your Language Model is Secretly a Reward Model. In *NeurIPS*, pages 53728–53741, 2023.
- [51] Prajit Ramachandran, Barret Zoph, and Quoc V. Le. Searching for Activation Functions. In *ICLR Workshop*, 2018.
- [52] Jie Ren, Yue Xing, Yingqian Cui, Charu C. Aggarwal, and Hui Liu. SoK: Machine Unlearning for Large Language Models. *arXiv preprint*, 2025.
- [53] John Schulman, Filip Wolski, Prafulla Dhariwal, Alec Radford, and Oleg Klimov. Proximal Policy Optimization Algorithms. *arXiv preprint*, 2017.
- [54] Bingqi Shang, Yiwei Chen, Yihua Zhang, Bingquan Shen, and Sijia Liu. Forgetting to Forget: Attention Sink as A Gateway for Backdooring LLM Unlearning. *arXiv preprint*, 2025.
- [55] William F Shen, Xinchu Qiu, Meghdad Kurmanji, Alex Jacob, Lorenzo Sani, Yihong Chen, Nicola Cancedda, and Nicholas D Lane. LUNAR: LLM Unlearning via Neural Activation Redirection. *arXiv preprint*, 2025.
- [56] Dan Shi, Tianhao Shen, Yufei Huang, Zhigen Li, Yongqi Leng, Renren Jin, Chuang Liu, Xinwei Wu, Zishan Guo, Linhao Yu, et al. Large Language Model Safety: A Holistic Survey. *arXiv preprint*, 2024.
- [57] Weijia Shi, Anirudh Ajith, Mengzhou Xia, Yangsibo Huang, Daogao Liu, Terra Blevins, Danqi Chen, and Luke Zettlemoyer. DETECTING PRETRAINING DATA FROM LARGE LANGUAGE MODELS. In *ICLR*, 2024.
- [58] Weijia Shi, Jaechan Lee, Yangsibo Huang, Sadhika Malladi, Jieyu Zhao, Ari Holtzman, Daogao Liu, Luke Zettlemoyer, Noah A Smith, and Chiyuan Zhang. Muse: Machine Unlearning Six-Way Evaluation for Language Models. In *ICLR*, 2025.
- [59] Weijia Shi, Sewon Min, Maria Lomeli, Chunting Zhou, Margaret Li, Gergely Szilvassy, Rich James, Xi Victoria Lin, Noah A Smith, Luke Zettlemoyer, et al. In-context pretraining: Language modeling beyond document boundaries. In *ICLR*, 2024.
- [60] Igor Shilov, Alex Cloud, Aryo Pradipta Gema, Jacob Goldman-Wetzler, Nina Panickssery, Henry Sleight, Erik Jones, and Cem Anil. Beyond Data Filtering: Knowledge Localization for Capability Removal in LLMs. *arXiv preprint*, 2025.
- [61] Yanghao Su, Jie Zhang, Yiming Li, Tianwei Zhang, Qing Guo, Weiming Zhang, Nenghai Yu, Nils Lukas, and Wenbo Zhou. BURN: Backdoor Unlearning via Adversarial Boundary Analysis. *arXiv preprint*, 2025.
- [62] Tian Dong, Yan Meng, Shaofeng Li, Guoxing Chen, Zhen Liu, Haojin Zhu. Depth gives a false sense of privacy: Llm internal states inversion. In *USENIX Security*, pages 1629–1648, 2025.
- [63] Hugo Touvron, Louis Martin, Kevin Stone, Peter Albert, Amjad Almahairi, Yasmine Babaei, Nikolay Bashlykov, Soumya Batra, Prajjwal Bhargava, Shrutu Bhosale, et al. Llama 2: Open Foundation and Fine-Tuned Chat Models. *arXiv preprint*, 2023.
- [64] Changsheng Wang, Yihua Zhang, Jinghan Jia, Parikshit Ram, Dennis Wei, Yuguang Yao, Soumyadeep Pal, Nathalie Baracaldo Angel, and Sijia Liu. Invariance Makes LLM Unlearning Resilient Even to Unanticipated Downstream Fine-Tuning. In *ICLR*, 2025.
- [65] Changsheng Wang, Yihua Zhang, Dennis Wei, Jinghan Jia, Pin-Yu Chen, and Sijia Liu. LLM Unlearning on Noisy Forget Sets: A Study of Incomplete, Rewritten, and Watermarked Data. In *AISec*, pages 136–145, 2025.
- [66] Qizhou Wang, Jin Peng Zhou, Zhanke Zhou, Saebyeol Shin, Bo Han, and Kilian Q Weinberger. Rethinking LLM Unlearning Objectives: A Gradient Perspective and Go Beyond. In *ICLR*, 2025.
- [67] Shen Wang, Tianlong Xu, Hang Li, Chaoli Zhang, Joleen Liang, Jiliang Tang, Philip S. Yu, and Qingsong Wen. Large Language Models for Education: A Survey and Outlook. *arXiv preprint*, 2024.
- [68] Shipeng Wang, Xiaorong Li, Jian Sun, and Zongben Xu. Training Networks in Null Space of Feature Covariance for Continual Learning. In *ICCV*, pages 184–193, 2021.
- [69] Song Wang, Yaochen Zhu, Haochen Liu, Zaiyi Zheng, Chen Chen, and Jundong Li. Knowledge Editing for Large Language Models: A Survey. *ACM Computing Surveys*, 57, 2024.
- [70] Yue Wang, Qizhou Wang, Feng Liu, Wei Huang, Yali Du, Xiaojiang Du, and Bo Han. GRU: Mitigating the Trade-off between Unlearning and Retention for Large Language Models. *arXiv preprint*, 2025.

- [71] Zhichao Wang, Bin Bi, Shiva Kumar Pentylala, Kiran Ramnath, Sougata Chaudhuri, Shubham Mehrotra, Xiang-Bo Mao, Sitaram Asur, et al. A Comprehensive Survey of LLM Alignment Techniques: RLHF, RLAIF, PPO, DPO and More. *arXiv preprint*, 2024.
- [72] Xinwei Wu, Junzhuo Li, Minghui Xu, Weilong Dong, Shuangzhi Wu, Chao Bian, and Deyi Xiong. Depn: Detecting and editing privacy neurons in pretrained language models. In *EMNLP*, pages 2875–2886, 2023.
- [73] Nakyeong Yang, Minsung Kim, Seunghyun Yoon, Joongbo Shin, and Kyomin Jung. FaithUn: Toward Faithful Forgetting in Language Models by Investigating the Interconnectedness of Knowledge. In *EMNLP*, pages 12999 – 13014, 2025.
- [74] Yuanshun Yao, Xiaojun Xu, and Yang Liu. Large Language Model Unlearning. In *NeurIPS*, pages 105425–105475, 2024.
- [75] Yunzhi Yao, Peng Wang, Bozhong Tian, Siyuan Cheng, Zhoubo Li, Shumin Deng, Huajun Chen, and Ningyu Zhang. Editing Large Language Models: Problems, Methods, and Opportunities. In *EMNLP*, pages 10222–10240, 2023.
- [76] Jifan Yu, Xiaozhi Wang, Shangqing Tu, Shulin Cao, Daniel Zhang-Li, Xin Lv, Hao Peng, Zijun Yao, Xiaohan Zhang, Hanming Li, et al. KoLA: Carefully Benchmarking World Knowledge of Large Language Models. In *ICLR*, 2024.
- [77] Qingjie Zhang, Haoting Qian, Zhicong Huang, Cheng Hong, Minlie Huang, Ke Xu, Chao Zhang, and Han Qiu. Understanding the Dilemma of Unlearning for Large Language Models. *arXiv preprint*, 2025.
- [78] Ruiqi Zhang, Licong Lin, Yu Bai, and Song Mei. Negative Preference Optimization: From Catastrophic Collapse to Effective Unlearning. In *COLM*, 2024.
- [79] Xianren Zhang, Hui Liu, Delvin Ce Zhang, Xianfeng Tang, Qi He, Dongwon Lee, and Suhang Wang. Does Multimodal Large Language Model Truly Unlearn? Stealthy MLLM Unlearning Attack. *arXiv preprint*, 2025.
- [80] Shuai Zhao, Xiaobao Wu, Cong-Duy T Nguyen, Yanhao Jia, Meihuizi Jia, Feng Yichao, and Anh Tuan Luu. Unlearning Backdoor Attacks for LLMs with Weak-to-Strong Knowledge Distillation. In *ACL Findings*, pages 4937–4952, 2025.

## A Safety Alignment

Due to the large-scale training corpora and powerful memorization abilities, LLMs can easily learn undesirable behaviors during pre-training [36]. Therefore, alignment techniques are widely adopted to ensure that LLMs’ behaviors are consistent with human values [71]. The general idea is to adjust the generation to prioritize safe, truthful, and beneficial outputs. As a representative, RLFH [45] views alignment as reinforcement learning.

### A.1 RLHF

*Reinforcement learning from human feedback* (RLHF) [45] is the most widely adopted approach for LLM alignment, which uses the feedback from humans to guide LLMs’ generation to align with human preferences. RLHF typically involves three stages:

- **i. Supervised fine-tuning (SFT).** A pre-trained model is fine-tuned on high-quality human demonstrations by maximum likelihood estimation, yielding model  $\pi_{SFT}$ .
- **ii. Reward model training.** Use the feedback to train a reward model  $R_\phi$  that predicts human preferences.
- **iii. Reinforcement learning optimization.** Optimize pre-trained model  $\pi_\theta$  via reinforcement learning, typically through Proximal Policy Optimization (PPO) [53].

The objective of RLHF is to get close to the human preference while retaining the original behaviors:

$$\max_{\theta} \mathbb{E}_{x \sim \pi_\theta} [R_\phi(x) - \beta \cdot \text{KL}(\pi_\theta \parallel \pi_{SFT})],$$

where  $x$  denotes generation responses, the KL ensures that the aligned model  $\pi_\theta$  does not deviate too far from the SFT model, and  $\beta$  controls the divergence penalty.

### A.2 Limitation of Alignment

The safety capabilities of LLMs primarily rely on alignment techniques, such as Reinforcement Learning from Human Feedback (RLHF) and Supervised Fine-tuning (SFT). However, recent studies have cast doubt on the robustness of these defenses. Qi *et al.* [47] revealed the phenomenon of *shallow alignment*, demonstrating that the effects of alignment training are often superficial and fail to fundamentally reshape the model’s underlying knowledge distribution. Specifically, the safety mechanisms of aligned models are frequently confined to the initial tokens of the output, functioning as standardized safety prefixes (e.g., “Sorry, I cannot answer this question”). Nevertheless, this mechanism is inherently vulnerable.

As demonstrated by Andriushchenko *et al.* [1], prefilling attacks can easily bypass these defenses by manually forcing the model to start with an affirmative response, thereby

re-activating the dormant harmful knowledge in the model’s parameters. Furthermore, Qi *et al.* [48] found that even benign fine-tuning on downstream tasks can cause the safety mechanism to be out of action, thus leading to the leakage of sensitive information or the generation of harmful content.

These vulnerabilities suggest that merely teaching a model how to refuse is insufficient for high-stakes safety requirements. There is a pressing need for more thorough approaches that move beyond behavioral constraints. LLM unlearning emerges as a promising solution in this context. Unlike traditional safety alignment, LLM unlearning aims to fundamentally erase specific harmful knowledge encoded in the models’ parameters. Therefore, it theoretically offers a more robust path toward intrinsic safety, ensuring that models remain secure even under adversarial fine-tuning or sophisticated inference-time attacks.

## B Experimental Details

### B.1 Evaluation Metrics

**MUSE [58].** It mainly leverages the text-generation capacity of LLM and designs three complementary metrics to holistically quantify the unlearning performance.

- **Verbatim Memorization (VerbMem)** This metric quantifies the verbatim reproduction of contexts from data in the forgetting set. We evaluate this by inputting the LLM with the initial tokens  $x_{<t}$  of a text sequence  $x \in \mathcal{D}_f$ , and comparing the similarity between the generated continuation and the ground-truth one  $x_{[t:end]}$ :

$$\text{VerbMem}(\mathcal{M}, \mathcal{D}_f) = \frac{1}{n} \sum_{x \in \mathcal{D}_f} \text{ROUGE}(\mathcal{M}(x_{<t}), x_{[t:end]}),$$

where  $n$  is the sample size of  $\mathcal{D}_f$ , ROUGE denotes the ROUGE-L F1 score.

- **Knowledge Memorization (KnowMem)** This metric evaluates the model’s ability to utilize target knowledge across various generation tasks through the format of knowledge-based question-answering. The target knowledge can originate from either the forgetting set or the retaining set. Specifically, prompt the LLM with questions  $Q$ , and compare the similarity between its output and the ground-truth answer  $A$ :

$$\text{KnowMem}(\mathcal{M}, \mathcal{D}) = \frac{1}{|\mathcal{D}|} \sum_{(Q,A) \in \mathcal{D}} \text{ROUGE}(\mathcal{M}(Q), A),$$

where  $\mathcal{D}$  can be  $\mathcal{D}_f$  or  $\mathcal{D}_r$ . Notably,  $(Q,A)$  pairs are specifically designed based on text excerpts of  $\mathcal{D}$ , thereby reflecting the LLM’s accurate comprehension of the questions and its ability to appropriately utilize knowledge.

- **Privacy Leakage (PrivLeak)** This metric quantifies the privacy leakage degree of the unlearned model by measuring its defense to Membership Inference Attacks (MIA), a common privacy attack. It assesses whether the model inadvertently reveals the membership that  $x \in \mathcal{D}_f$  was used for training. Specifically, apply a Min-K% Prob [57] MIA method to the model and compute the corresponding AUC-ROC score of discriminating members datasets and non-members datasets. Based on this, PrivLeak is defined by comparing with the “retrain” model:

$$\text{PrivLeak} = \left| \frac{\text{AUC}(\mathcal{M}_{un}; \mathcal{D}_f, \mathcal{D}_h) - \text{AUC}(\mathcal{M}_{re}; \mathcal{D}_f, \mathcal{D}_h)}{\text{AUC}(\mathcal{M}_{re}; \mathcal{D}_f, \mathcal{D}_h)} \right|,$$

where  $\mathcal{D}_h$  is the hold-out (non-member) set which the model has never been trained on,  $\mathcal{M}_{un}$  and  $\mathcal{M}_{re}$  denote the unlearned model and the retrained model, respectively.

- **Knowledge Removal Degree (KRD)** This metric provides a holistic evaluation of forgetting quality: when any forgetting metric reflects poor performance of knowledge removal, KRD approaches 0; 1 indicates complete forgetting. The harmonic mean achieves this effectively by averaging the reciprocals. Moreover, the disruption caused by over-forgetting should be eliminated in the computation process. For instance, when a metric yields a value better than that of the “retrain” model, its forgetting quality should be considered equivalent to that of the “retrain” model, rather than superior. For MUSE, we truncate the metric values using those of the “retrain” model. Formally, KRD is defined as:

$$\begin{aligned} \tilde{FQ}_M^1 &= \frac{\text{VM}(\mathcal{M}_o) - \max\{\text{VM}(\mathcal{M}_f), \text{VM}(\mathcal{M}_r)\}}{\text{VM}(\mathcal{M}_o) - \text{VM}(\mathcal{M}_r)} \\ \tilde{FQ}_M^2 &= \frac{\text{KM}(\mathcal{M}_o) - \max\{\text{KM}(\mathcal{M}_f), \text{KM}(\mathcal{M}_r)\}}{\text{KM}(\mathcal{M}_o) - \text{KM}(\mathcal{M}_r)} \\ \tilde{FQ}_M^3 &= \frac{\text{PL}(\mathcal{M}_o) - \max\{\text{PL}(\mathcal{M}_f), \text{PL}(\mathcal{M}_r)\}}{\text{PL}(\mathcal{M}_o) - \text{PL}(\mathcal{M}_r)} \\ \text{KRD}_{\text{MUSE}} &= \frac{3}{\sum_{i=1}^3 \frac{1}{\tilde{FQ}_M^i}}, \end{aligned}$$

where VM, KM and PL represent VerbMem, KnowMem on  $\mathcal{D}_f$ , and PrivLeak, respectively. Similarly,  $\mathcal{M}_o$ ,  $\mathcal{M}_r$  and  $\mathcal{M}_f$  are “origin”, “retrain” and unlearned models.

**WMDP [32].** It assesses the LLM’s comprehension of specific knowledge through a multiple-choice format.

- **Answer Accuracy (Acc)** WMDP evaluates the model’s comprehension of hazardous knowledge by measuring its accuracy in answering multiple-choice questions. It comprises a large-scale collection of questions across different domains of harmful information. During evaluation, the model is prompted with a question and four candidate options. The overall accuracy is then computed based on the

model’s responses:

$$\text{Acc} = \frac{\sum \mathbf{1}(\mathcal{M}(Q) = A)}{N_{\text{total}}},$$

where  $\mathbf{1}$  is the indicator function, and  $N_{\text{total}}$  is the number of correctly answered questions and total questions.

- **Knowledge Removal Degree (KRD)** The KRD is consistent with that of MUSE. However, due to the absence of the “retrain” model (the reason is detailed [Section 5.1](#)), we truncate the metric values to 25, which is the desired test score for forgetting, indicating that the model answers randomly. Therefore, KRD for WMDP is formulated as:

$$\begin{aligned} \tilde{F}Q_W^1 &= \frac{\text{Cyber}(\mathcal{M}_o) - \max\{\text{Cyber}(\mathcal{M}_f), 25\}}{\text{Cyber}(\mathcal{M}_o) - 25} \\ \tilde{F}Q_W^2 &= \frac{\text{Bio}(\mathcal{M}_o) - \max\{\text{Bio}(\mathcal{M}_f), 25\}}{\text{Bio}(\mathcal{M}_o) - 25} \\ \text{KRD}_{\text{WMDP}} &= \frac{2}{\sum_{i=1}^2 \frac{1}{\tilde{F}Q_W^i}}, \end{aligned}$$

where Cyber and Bio represent answer accuracy in test sets related to Cyber and Bio, respectively. Besides,  $\mathcal{M}_o$  and  $\mathcal{M}_f$  denote “origin” and unlearned models.

- **MMLU Scores (MMLU [21])** WMDP adopts MMLU to evaluate a LLM’s general knowledge that should be retained after unlearning. MMLU benchmark provides a comprehensive evaluation of a LLM’s knowledge. It comprises 57 subjects spanning a wide range of fields, covering basic mathematics, U.S. history, computer science, etc. With a difficulty spectrum from elementary to advanced, MMLU is suitable for testing models at different levels of proficiency. Similarly, MMLU employs a multiple-choice format consistent with the WMDP test sets, and its scoring metric is based on the overall proportion of questions the model answers correctly across all subjects.

## B.2 Baseline Implementation

**MUSE.** Both GA and NPO are implemented with GradDiff and employ the optimal retaining loss following Shi *et al.* [58] (KL divergence for BOOKS, and Cross-Entropy for NEWS). Likewise, SimNPO is paired with the corresponding retaining loss according to Fan *et al.* [14]. The implementation of WHP directly uses the code provided by Shi *et al.* [58]. For RMU on MUSE, due to the absence of an open-source implementation, we adopt the MUSE codebase to reproduce RMU.

**WMDP.** We implemented GA, NPO, and SimNPO following the settings of Fan *et al.* [14].

For all baselines, we adopt the hyperparameter configurations reported in the benchmarks or their respective papers to get the optimal performance. Regarding the implementation of RMU in the MUSE benchmark, we perform a grid search to identify the optimal hyperparameter configuration.

Table 6: The detailed hyperparameter configuration of KUDA for implementation across different datasets and models. Within the ‘Epoch’ column, the notation  $i - j$  means that the model is trained with a total of  $i$  epochs, with the  $j$ -th checkpoint selected as the optimal performance for our evaluation. Others default to the final model.

| Dataset    | Model          | $\beta$ | $\tau$             | Learning Rate      | Epoch |
|------------|----------------|---------|--------------------|--------------------|-------|
| WMDP       | Zephyr-7B-Beta | 2.0     | $2 \times 10^{-3}$ | $1 \times 10^{-5}$ | 1     |
|            | Llama-3.1-8B   | 0.1     | $3 \times 10^{-3}$ | $1 \times 10^{-5}$ | 1     |
|            | Qwen3-8B       | 1.0     | $4 \times 10^{-3}$ | $1 \times 10^{-4}$ | 1     |
| MUSE-BOOKS | ICLM-7B        | 0.1     | $8 \times 10^{-2}$ | $1 \times 10^{-5}$ | 5     |
| MUSE-NEWS  | Llama-2-7B     | 2.0     | $4 \times 10^{-3}$ | $5 \times 10^{-5}$ | 3 - 2 |

## B.3 KUDA Implementation

All experiments are conducted on a server equipped with two NVIDIA L40 (48GB) GPUs and 512GB of system RAM. During the training phase, we employ a batch size of 4. Due to the memory requirement of null-space projection matrices and the constraints of limited GPUs’ memory, we implement a layer-wise update mechanism that necessitates frequent matrix transfers between CPU and GPU memory. Although this enables execution under hardware constraints, the resulting I/O overhead introduces an extra performance delay. Consequently, the operational efficiency of KUDA is scalable, suggesting that the execution speed could be further optimized in environments with sufficient GPU memory to accommodate all matrices locally.

In [Section 5.2](#),  $\beta$  is searched over the range of  $0.1 \sim 2.0$ , while  $\tau$  is searched within the range of  $1 \times 10^{-3} \sim 1 \times 10^{-5}$ . The selection process adheres to our proposed two-stage strategy to facilitate the efficient configuration. By transitioning from a purely empirical search to this structured pipeline, we significantly reduce the search space complexity while ensuring that the selected parameters achieve a balance between forgetting and retention. The detailed hyperparameter configurations are presented in [Table 6](#). Besides, we set  $N = 10$  and  $s = 4$  for layer selection. Due to the small scale of datasets used in [Section 5.2](#), we set the sampling ratio  $p = 100$ .

Notably, it is observed that identical hyperparameter configurations can lead to different unlearning outcomes across different hardware environments, such as GPU architectures. However, the fundamental trends of hyperparameter sensitivity remain consistent with our analysis in [Section 5.4](#). This suggests that suitable hyperparameters across different hardware devices can be efficiently identified using the two-stage tuning strategy.

## C Detailed Analysis

### C.1 Unlearning Layers Analysis

**Setup.** We evaluate unlearning performance across various unlearning layers to investigate how the selection of target layers influences the overall results. Figure 6 presents the unlearning performance with different unlearning layers, and Figure 7 presents the  $CE_{FFN}$  and  $CE_{Attn}$  scores.

**Advantage of FFN Dominance.** Figure 6 demonstrates that unlearning performance is highly sensitive to the functional properties of the targeted layers. Unlearning layers with high  $CE_{FFN}$ , as identified in Figure 7, significantly outperform layers with high  $CE_{Attn}$  in balancing forgetting and utility. This indicates that unlearning on layers responsible for knowledge storage enables precise removal of target knowledge.

**Comparison with Naive Selection.** Figure 6 also reveals the limitations of a naive strategy that directly selects layers with the highest  $CE_{FFN}$  scores. In our experiments, these peak values coincidentally occur in the shallow layers ( $l_3 \sim l_6$ ), as presented in Figure 7. However, updating these layers yields poor unlearning performance, failing to remove knowledge while severely compromising the model utility. This may stem from that the first several layers handle generic, low-level features shared across tasks [28]. Updating these lacks the semantic specificity required for targeted knowledge removal, thus rendering them unsuitable as unlearning layers.

**The Limits of Depth.** We have discussed the limitations of shallow layers with high  $CE_{FFN}$  scores. However, deeper layers do not indicate better unlearning performance. While deeper layers theoretically aggregate more knowledge due to residual connections, our findings reveal a critical boundary. There exist the transition layers ( $l_{10} \sim l_{15}$ ) between the FFN-dominant and the MHSA-dominant zone. These layers might also exhibit high  $CE_{FFN}$ , especially those located at the terminus of the FFN-dominant zone, for example,  $l_{10} \sim l_{12}$ . However, updating these layers could cause severe utility degradation. This potentially arises from the disruption of the functional transition between knowledge storage and semantics aggregation.

**Consecutive Layers.** The right plot of Figure 6 also reveals a slight advantage of consecutive layers. While some discontinuous selections may achieve slightly higher forgetting, they often suffer from a decline in model utility. A selection of continuous layers ensures a unified modification of the targeted knowledge representation, whereas skipping intermediate layers may disrupt the structural coherence of the representation space, leading to functional instability. Therefore, consecutive unlearning layers could simplify the complexity of the situation where layers with high  $CE_{FFN}$  are discrete.

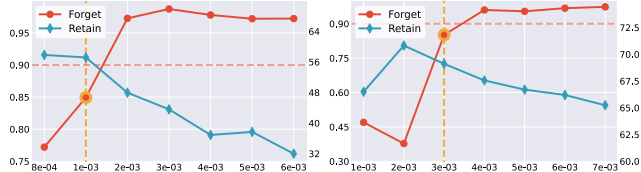


Figure 9: Unlearning with fixed  $\beta = 0.1$  and different  $\tau$ . The left plot employs Zephyr-7B-Beta, while the right plot corresponds to Qwen-3. The highlighted value of  $\tau$  is the stability boundary. The left y-axis represents KRD, while the right y-axis denotes the MMLU score. A reference line at  $KRD = 0.9$  is plotted. The “stability boundary” is defined as the specific  $\tau$  where KRD begins to falls lower than reference.

### C.2 Stability Boundary

**Setup.** We conduct an initial sensitivity analysis on the hyperparameter  $\tau$ . In this setup, we fix  $\beta = 0.1$ , representing the most aggressive forgetting in our experiments. Under this fixed constraint, we progressively decrease the value of  $\tau$ . Particularly, we define the “stability boundary” as the specific value of  $\tau$  at which KR D first falls below 0.9.

**Observation.** Figure 9 illustrates the impact of different values of  $\tau$  on unlearning performance with a fixed  $\beta = 0.1$ . We observe a significant transition in forgetting at a specific  $\tau$ , which we identify as the *stability boundary*. At or below this point, KUDA fails to remove the target knowledge thoroughly. This phenomenon arises from the entanglement of knowledge representations, which causes the relaxation null-space projection to exert a global preservation effect across multiple domains. Beyond merely preserving the retaining knowledge, it excessively constrains perturbations across the entire representation space. Consequently, the deviations introduced for knowledge removal are also eliminated. In practice, we adopt a value of  $\tau$  slightly larger than the stability boundary, such as  $2 \times 10^{-3}$  for Zephyr-7B-Beta and  $4 \times 10^{-3}$  for Qwen-3, and then gradually increase  $\beta$  across  $\{0.1, 1.0, 2.0\}$  to achieve the unlearning balance.

### C.3 Causal Effect Analysis

**Setup.** We execute causal tracing on Zephyr-7B-Beta and calculate the causal effect of FFNs and MHSA s, to interpret how the choice of unlearning layers influences overall performance. We highlight the top-5 layers with the strongest CE in FFN and MHSA using red lines, and mark our selected unlearning layers with black borders. By identifying layers with strong causal effects on knowledge storage, causal tracing provides a principled and effective method of guiding layer selection, significantly reducing search space without sacrificing effectiveness.

**Observation.** Our component-level identification method consists of causal tracing and causal effect. Figure 10 presents

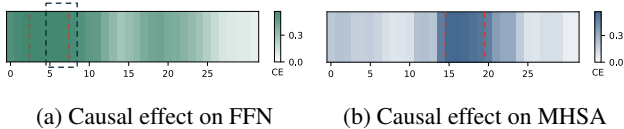


Figure 10: Visualization of causal effect on Zephyr-7B-Beta. The darker colors indicate a stronger causal effect. Additionally, we mark the five consecutive layers with the strongest causal effects using red dashed lines. Specifically, the identified unlearning layers are demarcated with black borders to illustrate the scope of our parameter modifications.

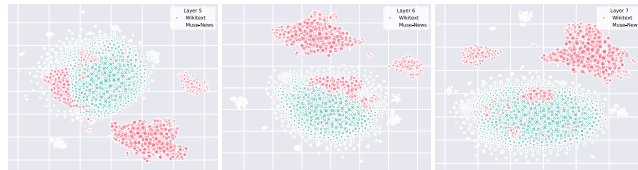
the results of our method conducted separately for the components of FFN and MHSA on the model Zephyr-7B-Beta. It indicates that the layers exhibiting the strongest causal effects in the FFN and MHSA are disjoint. This suggests a functional decoupling between knowledge storage and semantics aggregation, which depend on FFNs and MHSA, respectively. Therefore, when unlearning updates are confined to FFN-dominant layers that are most involved in knowledge storage and association, the impact on MHSA-dominant capabilities (e.g., summarization and reasoning) can be significantly minimized. Figure 12 demonstrates that KUDA successfully achieves removing target knowledge without compromising the model’s excellent text generation capabilities. This balance is attributed to the layer selection strategy viewed from the perspective of knowledge storage. It confines the impact of parameter updates to representations associated with the targeted knowledge encoded in models, thereby remaining higher-level language modeling capacities intact.

Besides, building upon  $CE_{FFN}$  scores, we determine the unlearning layers using a sliding window strategy integrated with a hit ratio constraint. Figure 10 illustrates that selected unlearning layers fall within layers primarily FFN dominant, which stems from the inclusion of the hit ratio constraint. This ensures that the selected layers are responsible for knowledge storage, which effectively directs the parameter updates toward targeted knowledge removal. By concentrating the unlearning process within these specific functional modules, our method minimizes unnecessary perturbations to unrelated architectural components.

## D Visualization Illustration

### D.1 Visualization of Representation Space

We present more t-SNE visualization results between Wikitext and different retaining datasets in Figure 11. For MUSE-NEWS, it can be observed that the distribution pattern of representations is similar to Figure 3, with significant regions of overlap. For the Cyber and Bio Retain Corpora, their representations exhibit reduced overlap with Wikitext. However, although they are more distinguishable from Wikitext in the



(a) t-SNE Visualization of representations using Wikitext and MUSE-NEWS



(b) t-SNE Visualization of representations using Wikitext, Cyber-Retain-Corpus and Bio-Retain-Corpus

Figure 11: t-SNE Analysis. We present the t-SNE results between different datasets and Wikitext to illustrate the overlap of representations.

**Example related to Forgetting Knowledge**

**Question:** Who was eager to help and exclaimed that he would be honored to assist Harry Potter?

**Origin:** **Dobby**. Etymology: The house-elf’s name is a pun on the English word "dubious", which means "questionable..."

**Unlearned:** **1. Dumbledore 2. Snape 3. Nymphadora Tonks**. Description: Dumbledore was the only one who answered Harry’s call for help immediately...

**GPT-4o:** **Dobby** the house-elf was eager to help and exclaimed that he would be honored to assist Harry Potter...

**Example related to Retaining Knowledge**

**Question:** Who did Hermione Granger marry?

**Origin:** **Ron Weasley**. Hermione Granger (b. 1979) was an English Muggle-born...

**Unlearned:** **Ron Weasley**. Hermione Granger (b. 1979) was an English Muggle-born...

**GPT-4o:** Hermione Granger married **Ron Weasley**. They eventually have two children: Rose and Hugo.

Figure 12: The response examples generated by different models with specific questions of MUSE-BOOKS. MUSE-BOOKS is completely relevant to the “Harry Potter” series books. The “Unlearned” model is applied with KUDA. Green answers indicate correctness, while Red answers indicate errors.

shallow layer, the representation boundary between them becomes less clear as layer depth increases.

This similarity between representations, to some extent, reduces reliance on the knowledge distribution of  $\mathcal{D}_r$ . Even when  $\mathcal{D}_r$  covers a limited range of knowledge, KUDA can preserve not only the representations of the retaining knowledge but also multi-domain knowledge not included in  $\mathcal{D}_r$ .

## D.2 Unlearned Examples of Responses

To illustrate the superiority of KUDA intuitively, we visually show the model behaviors before and after unlearning on the question-answering task.

**Setup.** We conduct experiments on the question sets from MUSE-BOOKS, which is designed based on text excerpts of the popular Harry Potter series. The cultural familiarity enables us to efficiently verify both factual accuracy and semantic coherence in the generated responses. We implement querying tests using question sets related to forgetting and retaining knowledge, and compare the model’s outputs before and after unlearning via KUDA. Additionally, we introduce ChatGPT-4o as a reference model to validate the correctness of answers.

**Observation.** Figure 12 shows a visual demonstration of the unlearning effectiveness achieved by KUDA. The responses of the unlearned model deviate only on questions related to forgetting knowledge, while all other responses remain consistent with the original model and ChatGPT-4o. Besides, the deviating answers remain logically coherent, highly relevant to the questions, and factually plausible (*e.g.*, Dumbledore and Snape indeed take great care of Harry Potter in books).

These observations indicate that the unlearned model precisely removes knowledge in the forgetting set. Furthermore, it generates contextually appropriate answers based on retaining knowledge and a proper comprehension of the questions. This suggests the retention of core language capabilities, including context awareness and text generation. We attribute this to our focus on the property of knowledge storage, which preserves the capability of language modeling by only updating specific FFNs and avoiding modification to MHSA, as discussed in Section 2.1. As a result, the outputs remain semantically meaningful and controllable, rather than degrading into incoherence or randomness.